NASA CR 72441

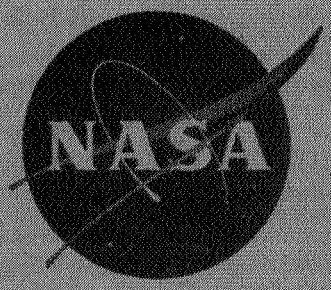

DYNAMIC LIQUID/SOLID CONTACT ANGLES AND FILMS ON CONTAMINATED MERCURY

by

Alfred H. Ellison and Silvestre B. Tejada

Prepared for

National Aeronautics and Space Administration

July 23, 1968

Contract NAS 3-9705

GILLETTE RESEARCH INSTITUTE, INC.
Harris Research Laboratories Division
1413 Research Boulevard
Rockville, Maryland 20850

NASA CR 72441

Final Report

DYNAMIC LIQUID/SOLID CONTACT ANGLES AND FILMS ON CONTAMINATED MERCURY

by

Alfred H. Ellison and Silvestre B. Tejada

Prepared for

National Aeronautics and Space Administration

Contract NAS 3-9705

Technical Management
NASA Lewis Research Center
Cleveland, Ohio
Spacecraft Technology Division
Donald A. Petrash

GILLETTE RESEARCH INSTITUTE, INC.
Harris Research Laboratories Division
1413 Research Boulevard
Rockville, Maryland 20850

DYNAMIC LIQUID/SOLID CONTACT ANGLES AND FILMS ON CONTAMINATED MERCURY

by

Alfred H. Ellison and Silvestre B. Tejada

ABSTRACT

Dynamic contact angle data were obtained for selected combinations of seven liquids and five solids. The contact angle increases with increasing velocity and depends largely on the properties of the liquid. The effect of solid substrate is small but significant, especially at low velocities. Individual data fit the equation $\theta = A \tanh CV + D\sqrt[3]{V}$ where θ is the contact angle, V, the velocity and A, C and D are coefficients dependent on liquid-solid properties.

Surface films from mercury contaminated with a trace of soluble metal contain, as a major constituent, the metal contaminant. The films apparently are oxides of contaminants. The surface potential of mercury changes when soluble metals are added.

SUMMARY

Dynamic contact angle data were obtained for selected combinations of seven liquids and five solids. The dynamic contact angle increases with increasing liquid-solid relative velocity and is observed to depend largely on the properties of the liquid. Viscosity and surface tension of the liquid have the most influence in the variation of liquid-solid dynamic contact angle. The effect of the solid substrate is small but real, especially at low relative velocities.

Individual liquid-solid data were found to fit the equation $\theta = A \tanh CV + D\sqrt[3]{V}$ where θ is the dynamic contact angle at velocity V and A, C and D are coefficients related to the properties of the liquid-solid systems. The precise relationships, however, have not yet been established.

The films which form on the surface of mercury containing 2 ppm of soluble metal contaminants contain, as a major constituent the contaminant metal. Oxidized mercury is a minor constituent. The surface potential of mercury changes rapidly when these soluble metal contaminants are added. These results demonstrate high surface activity of soluble metal contaminants in mercury; that is, the contaminant diffuses rapidly to the surface and tends to concentrate there. In the case of zinc and lead, there is evidence that the contaminant reacts with atmospheric oxygen at the surface to form the corresponding oxide. The other soluble contaminants probably followed the same procedure. It is likely that the scum frequently observed on the surface of mercury is an accumulation of insoluble contaminant oxides. In situations where oxygen or other reactive gases could be absolutely excluded one could speculate that soluble metal contaminants would be concentrated at the surface of mercury. Thus any uses of mercury in which the behavior depends upon its surface properties can be expected to be affected by trace metal contaminants.

INTRODUCTION

Previous work for the Spacecraft Technology Division of the NASA Lewis Research Center carried out at the Gillette Research Institute has involved studies of various aspects of the problem of the wetting of solid surfaces by liquids[1,2,3]. This information is used by NASA in dealing with the problem of handling and storing liquids in spacecraft under zero-gravity conditions. The work reported here comprises two further aspects of wetting phenomena. One concerns the dynamic contact angle formed by a liquid as it advances over the surface of a solid. The objective of this phase of the work was to devise a mathematical expression from which a dynamic contact angle could be calculated for a given system from a knowledge of the relative velocity of the liquid over the solid and the appropriate properties of the liquid and the solid. To achieve this objective the plan was to obtain dynamic contact angle data for a variety of liquid-solid systems covering a wide range of liquid and solid properties, which would be used as the basis for the mathematical formulation.

The wetting of solid surfaces by mercury involves problems not encountered with other liquids and is justifiably considered separately. The very high contact angles shown by mercury on most solid surfaces and the susceptibility of the mercury surface to contamination are the bases of these unique problems. Aspects of these problems have been the subjects of earlier phases of work for the Spacecraft Technology Division here at the Gillette Research Institute. In this earlier work it was established that trace amounts of soluble metallic impurities had an enormous effect on the surface properties of mercury. In most cases a film formed on the surface of mercury which over a period of time or with appropriate sweeping of the surface developed into the visible scum familiar to those who have had occasion to work with mercury. It was important to understand the effect of trace contaminants on the surface properties of mercury because that which affects the surface properties of mercury will also affect the wetting by mercury of solid surfaces. The object of this work was therefore to analyze the surface film which forms on mercury containing trace

contaminants. By doing so it should be possible to understand and bring under control the effect of trace metal contaminants on the surface properties of mercury.

The two phases of work involved two groups of Tasks and are reported as such below.

In addition to the authors the following people contributed to this work: Dr. Anthony M. Schwartz, Mr. John D. Galligan, Mr. R. Bruce Klemm, Mr. George A. Lyerly, Mrs. Helen Y. Hsiao, Mr. Laszlo Hogye and Mr. Plato Watts.

FILMS ON CONTAMINATED MERCURY

TASK I - EXPERIMENTAL TECHNIQUE FOR THE ISOLATION AND COLLECTION OF SURFACE FILMS ON MERCURY

I. INTRODUCTION

It is the purpose of this task to develop an experimental technique for isolating and collecting the surface films formed at the vapor-liquid interface of mercury upon addition of trace amounts of soluble contaminants. The method finally adopted is based on a sweeping barrier technique in the manner described by Ellison[4].

II. EXPERIMENTAL

A. Materials

The materials required for this task and succeeding tasks are tabulated in Appendix I.

B. Purification of Mercury

Detergent-washed mercury was passed several times down a column of 10% nitric acid solution in a Thomas-John Mercury Cleaning Apparatus*. The apparatus consists of a glass cleaning column which can be filled with suitable cleaning agent and a filter tube to which a polyethylene screw cap with a stainless steel screen is attached. The purpose of the latter is to break the mercury into tiny cascading globules to expose maximum mercury surface to the cleaning agent. The acid treatment was repeated with at least three changes of the nitric acid solution. Rinsing of the acid treated mercury was done in the same apparatus with the column filled with double-distilled water. The water in the column was changed at least three times during the process. The mercury was then dried by passing it through a small hole in the tip of an ashless filter paper. The process was repeated using a dry filter paper for each repetition until no visible water remained

*Manufactured by Arthur H. Thomas Company of Philadelphia.

on mercury and the filter paper showed no visible wetting. The mercury was then distilled under vacuum in a CENCO mercury still at the rate of about one pound of mercury per hour and collected and stored in clean polyethylene bottles.

C. Apparatus

(1) A rectangular trough (2" x 4" x 1/4" deep) was fabricated from Plexiglas and was capable of holding about 500 grams of mercury. The mercury surface is "framed" by a 1 mil Mylar film attached to the trough edges and which extends not less than 1/8 inch over the mercury surface from the edge of the trough. The Mylar film is held in place by adhesive tape.

(2) Sweeping barriers were 4" x 1/2" strips of 1 mil Mylar film glued for support onto the entire length of 1/2" x 1/4" x 4" brass frame by adhesive tape. A complete set-up is shown in Figure 1.

D. Isolation and Collection of Surface Film

The isolation and collection of surface films on mercury were done inside a dry box where the oxygen content was maintained below the 0.2% level by flushing the box with dry ultra-high purity nitrogen. The box atmosphere was repeatedly analyzed during the isolation and collection process by gas chromatography using an F and M Model 500 gas chromatograph equipped with a thermal conductivity detector and 5X molecular sieve column.

The Plexiglas trough was filled inside the dry box with about 500 grams of freshly-distilled mercury until the mercury level was slightly above the plane of the trough. At this point the Mylar film frame and the sweeping barriers adhered tightly to the mercury surface providing a tight surface seal.

The mercury surface was swept along the length of the trough using the Mylar sweeping barrier and swept a second time after a half-minute wait to ascertain that the mercury was of acceptable purity. The presence of base impurities is manifested by visible surface film wrinkling in the area in front of the sweeping barrier (see Figure 2).

A pre-weighed amount of fresh zinc shavings, enough to make 2 ppm solution when mixed with the mercury in the trough, was dissolved in 1 ml of mercury in a plastic covered vial and then poured quickly into the bulk mercury in the trough. The mercury surface was swept unidirectionally along the length of the trough with the barrier given a slight to-and-fro motion perpendicular to the direction of sweeping. The surface film was collected at the end of each sweep with the aid of a small Mylar strip.

To collect enough of the material for analysis, it was necessary to replenish the contaminant in the trough after repeated sweepings.

E. Removal of Entrained Mercury

Microscopic examination of raw surface film showed a large amount of entrained mercury globules (see Figure 3). The amount of entrained mercury was significantly reduced by subjecting the raw film in a plastic covered vial to a vigorous mechanical shaking in a dental amalgamator.* By this process the mercury globules coalesce to form larger globules and separate from the bulk of the powdery material. Mechanical shaking was repeated until no more liquid mercury could be separated.

F. Analysis of Refined Surface Film

The refined film was subjected to X-ray powder analysis, selected area electron diffraction analysis and wet chemical analysis. A brief description of these analytical techniques is presented in Appendix II.

III. RESULTS AND DISCUSSION

Zinc-contaminated mercury was used in the development of this technique. The X-ray powder photograph of the refined film samples from zinc-contaminated mercury showed definite crystalline patterns of zinc oxide. This identification was also confirmed by selected area electron diffraction analysis.

---

*Manufactured by Crescent Dental Manufacturing Company.

Chemical analysis of the refined film using the dithizone method[5] showed 61% zinc and 0.7% oxidized mercury. The remainder presumably comprised metallic mercury and oxygen with the latter in the form of metal oxides. These procedures established the validity of the technique.

The rate of formation of the surface film was very rapid even with the dry box atmosphere maintained at below 0.2% oxygen. The amount of surface film collected diminished with continued sweepings, indicating depletion of the contaminant in the bulk mercury.

IV. CONCLUSION

The technique of using plastic film barriers to manually sweep surface films from contaminated mercury, followed by vigorous agitation to coalesce entrained mercury is an effective, although tedious and time consuming method of isolating for analysis films from the surface of contaminated mercury. Typical wet chemical or crystallographic analyses can then be performed on the samples.

TASK II - APPLICATION OF TASK I TECHNIQUE TO PURE MERCURY AND TO MERCURY CONTAMINATED WITH ZINC AND LEAD

I. INTRODUCTION

The object of this task is to apply the technique developed under Task I to systems of pure mercury, zinc-contaminated and lead-contaminated mercury. An additional requirement for Task II is the measurement of the surface tension of purified mercury to index its purity. A maximum bubble pressure apparatus patterned after Sugden[6] was designed and constructed for this purpose.

II. EXPERIMENTAL

A. Materials

All materials used in this task are tabulated in Appendix I. Mercury samples used in the experiment had surface tension of 473 $\pm$ 10 dynes/cm.

B. Apparatus

(1) A maximum bubble pressure apparatus was fabricated and is shown in Figure 4. The radii r_1 and r_2 of the capillary jets were 0.062 and 0.1273 cm respectively.

(2) A 24 x 5 x 1/4 inch Plexiglas trough framed with 1 mil Mylar film and equipped with a suitable Mylar sweeping barrier was used to collect surface films from pure mercury. The collection of surface films from contaminated mercury made use of the troughs and barriers developed in Task I.

C. Measurement of Surface Tension

Measurements of surface tension were made using dry nitrogen as the bubbling gas. The depths of immersion of the capillary jets were so adjusted that the bubbling gas escaped at the same rate at both jets, with the nitrogen pressure maintained constant. Under this condition the surface tension of the liquid is given by:

$$\gamma = \frac{gd}{2} (t_2 - t_1) \left(\frac{1}{r_1} - \frac{1}{r_2} \right)$$

where

γ = surface tension

g = gravitational constant

d = density difference between the liquid and the gas

r_1 and r_2 = radii of capillary jets 1 and 2, respectively

t_1 and t_2 = immersion depths of capillary jets 1 and 2, respectively

Final calculations of the surface tension were performed in the manner described by Bosworth[7]. The immersion depths were measured with a cathetometer with attainable reproducibility of $\pm$ 0.01 cm. The immersion depth is defined here as the distance between the mercury planar surface and the capillary tip.

D. Isolation, Collection and Analysis of Surface Films

The techniques employed for the isolation, collection and refining of surface films from pure mercury and mercury contaminated with zinc and lead were those developed in Task I. For the collection of surface films resulting from normal oxidation of mercury it was necessary to expose a large mercury surface to reduce collection time. For this purpose, a 24 x 5 x 1/4 inch Mylar-framed Plexiglas trough equipped with a suitable Mylar sweeping barrier was used.

The refined samples from pure, zinc-contaminated and lead-contaminated mercury were analyzed by X-ray powder analysis and by the dithizone method. The surface film from pure mercury was scanned polarographically for possible presence of metallic contaminants using a Fisher Electropode Model 65 (see Appendix II).

III. RESULTS AND DISCUSSION

Chemical analysis of the refined film from zinc-contaminated mercury showed 61% zinc and 0.7% oxidized mercury. The remainder presumably comprised metallic mercury and oxygen in the form of metallic oxides.

That the surface film forming on the vapor-liquid interface of mercury contaminated with trace amount of zinc is probably an oxide is supported by the results of a side experiment. When about 1 mg of zinc was added to 10 ml of mercury under vacuum, the zinc dissolved without any visible effect on the surface appearance of mercury even after vigorous shaking, and no skin or film was observed to form. Admission of air into the system was followed by immediate dulling of the mercury surface and the formation of a coherent film. The film can be observed as surface wrinkles by tilting the glass container. Shaking the container resulted in the formation of a black powdery residue.

Earlier samples of films from zinc-contaminated mercury showed amorphous X-ray powder patterns. Microscopic examination of the film showed, however, that it contained entrained free mercury globules. This large excess of free mercury is believed to have completely obscured the crystalline pattern of zinc oxide. Positive identification of zinc oxide was obtained by X-ray analysis from samples further refined by vigorous mechanical shaking with a dental amalgamator.

Lead dissolved very readily in mercury followed by immediate formation of a surface film. The film was more coherent than that resulting from zinc contamination and moreover, a much larger amount of greyish-black raw film was collected for the same weight of the metal contaminant. Microscopic examination of the film showed a larger amount of entrained mercury. The supply of the film was seemingly inexhaustible and it took more sweepings before the amount of film collected per sweep was significantly reduced.

The refined film was greyish-black and gave a diffuse and rather complex X-ray powder pattern. Closer examination of the X-ray powder

photographs showed identifiable amounts of lead monoxide (PbO). A similar result was obtained from selected area electron diffraction analysis. Although other crystalline forms of oxides of lead are suggested by the powder pattern, attempts at positive identification of the crystalline forms were unsuccessful. The bulk of the refined film is believed to be amorphous, most probably in the form of lead sub-oxide (Pb_2O). The result of the wet chemical analysis for lead (96% lead, 2.5% Hg^{++}) and the diffuse character of the X-ray powder pattern, lend support to the above deduction.

The formation of a surface film on the vapor-liquid interface of pure mercury under dry box conditions was extremely slow despite a large surface area exposed to the atmosphere. The interval between successive sweeps had to be 24 hours in order to collect a reasonable amount of film. It took 2-1/2 months to collect enough refinable surface film for the X-ray analysis.

The refined film gave amorphous X-ray powder patterns. Polarographic scan of the refined film using 6N HCl as supporting electrolyte, showed oxidized mercury as the main constituent. Wet chemical analysis using dithizone method gave 5.4% oxidized mercury (Hg^{++}). A trace amount of lead was also indicated. The remainder was presumably unoxidized entrained mercury.

The purified mercury used in this work was found to have a surface tension of 473 $\pm$ 10 dynes/cm. The good agreement between this value and the published value of 485 dynes/cm shows the effectiveness of the purification procedure.

IV. CONCLUSIONS

The films which form on the surfaces of zinc-contaminated and lead-contaminated mercury contain zinc and lead, respectively, as the main constituents. For the most part these are present as oxides. A film forms on purified mercury only very slowly. The main constituent of this film is mercury.

TASK III - EFFECTS OF OTHER IMPURITIES ON SURFACE PROPERTIES OF MERCURY - SURFACE POTENTIAL

I. INTRODUCTION

The surface films on the liquid-vapor interface of mercury containing 2 ppm of other soluble contaminants were collected, refined and analyzed by the method developed in Task I. The surface potentials of the contaminated mercury were measured using an air ionization electrode in a manner described in a previous report[1].

II. EXPERIMENTAL

A. Materials

The materials used in this task are tabulated in Appendix I.

B. Apparatus

(1) All apparatus fabricated in Task I and II were used in this Task.

(2) A radium ionization electrode, a Keithley Electrometer Model 610BR, and a Sargent Model MR potentiometric recorder were used in the measurement of surface potential.

C. Isolation, Collection and Refining of Surface Film

Attempts were made to dissolve 2 ppm of nickel, silver, copper, bismuth, tin and rubidium in mercury. The surface films which formed were collected, refined and analyzed by the method developed in Task I.

D. Surface Potential Measurement

The troughs for the surface potential measurement were shallow 3-inch plastic Petri dishers. A 4-inch diameter circular sheet of 1 mil Mylar film was placed on top of each dish and glued underneath to the sides of the dish with adhesive tape. One and three cm^2 openings were cut on the Mylar film to provide electrode access to the mercury.

The contaminants needed to make 2 ppm solutions were predissolved in mercury in a 50 ml Erlenmeyer flask inside the dry box and the mixture poured into the Petri dish through the large opening. The surface potentials were then measured in the manner described in a previous report[1]. The potentials of the following systems were measured: pure mercury, silver-, copper-, bismuth-, tin-, and rubidium-contaminated mercury.

III. RESULTS AND DISCUSSION

A. Analysis of Surface Films

Nickel: Nickel did not dissolve in mercury even under vacuum at elevated temperature. No film was observed to form on the surface of mercury.

Silver: Silver dissolved readily in mercury. However, no visible changes were observed on the mercury surface nor could any surface film be collected even after a 24-hour wait.

Copper: Copper, although seeming to amalgamate readily, dissolved very slowly in mercury. The rate of formation of the surface film was likewise slow. Even further addition of a fresh charge of copper predissolved in mercury under vacuum at elevated temperature did not increase significantly the rate of film formation. The film was very thin and did not have the coherence exhibited by films from lead-contaminated and zinc-contaminated mercury.

The refined film was found to contain 4.7% copper by polarographic analysis and 3.5% oxidized mercury (Hg^{++}) by the dithizone method. No other metallic contaminant was detected. The bulk of the refined film was presumed to be free mercury which could not be separated from the oxide skin by the refining technique developed in Task I. The X-ray powder photograph of the refined film gave an amorphous pattern, most probably due to the presence of a large excess of free mercury.

Bismuth: Bismuth dissolved very readily in mercury and the solution was followed by immediate formation of surface film. The refined film was found to contain 8.7% bismuth and no other detectable metallic contaminant

by polarographic techniques. Chemical analysis of the refined film for oxidized mercury (Hg^{++}) using the dithizone method gave 1.5% Hg^{++}. The bulk of the film, as in the case of the film from copper contaminated mercury, was presumably free mercury. The X-ray powder photograph of the refined film showed an amorphous pattern. It is reasonable to assume, as was found in the cases of films from zinc-contaminated and lead-contaminated mercury, that the surface film was an oxide or mixed oxides of bismuth.

Tin: The reaction of tin with mercury was very similar to that of bismuth. It dissolved very readily in mercury with immediate formation of surface film. The refined film was greyish-black, slightly lighter in color than the film collected from bismuth-contaminated mercury. It was found to contain 12% tin by polarographic analysis and 2.5% oxidized mercury (Hg^{++}) by the dithizone method. No other metallic contaminant was detected. The bulk of the film was again presumed to be free mercury which could not be removed by the separation technique developed in Task I. The X-ray powder analysis of the refined film sample showed it to be amorphous.

Rubidium: Rubidium was found to react rapidly with air even though the oxygen content of the dry box atmosphere was brought down below the 0.1% level. Its bright mirror-like surface was instantly tarnished when the vacuum sealed glass container was broken inside the dry box.

Rubidium dissolved readily in mercury with an accompanying formation of a thin film on the mercury surface. The film lacked the coherence of films resulting from soluble contaminants mentioned previously. No significant amount of film could be isolated by the technique developed in Task I. The film adhered to the Mylar film barrier during the sweeping process. Although no film was collected for analysis, there is strong reason to believe, from the known reactivity of rubidium, that the film was essentially an oxide, or mixed oxides.

A summary of the analyses of surface films from contaminated mercury is given in Table I.

B. Surface Potentials

The results of the surface potential measurements on pure mercury and mercury contaminated with copper, tin, bismuth and rubidium, together with the previous measurements on mercury containing trace of zinc and lead are summarized in Table II. Of the four contaminants studied, only copper gave a positive surface potential with respect to that of freshly distilled mercury. Although no quantitative interpretation of the surface potential values could be advanced at this time, the results nevertheless show the sensitivity of the surface potential of mercury to the presence of trace amounts of soluble contaminants.

DISCUSSION OF WORK ON FILMS ON CONTAMINATED MERCURY

The results from the studies of Tasks II and III demonstrate a high level of surface activity of soluble metal contaminants in mercury. That is to say that the contaminant diffuses rapidly to the surface and tends to concentrate there. In the case of zinc and lead there is evidence that the contaminant reacts with atmospheric oxygen at the surface to form the corresponding oxide. The other soluble contaminants probably followed the same procedure but did not form large enough crystalline aggregates in the isolation and refinement procedures to yield an X-ray or electron diffraction pattern. It is likely that the scum frequently observed on the surface of mercury is an accumulation of insoluble contaminant oxides. In situations where oxygen or other reactive gases would be absolutely excluded one would speculate that soluble metal contaminants would be concentrated at the surface of mercury. Thus, any uses of mercury in which the behavior depends upon its surface properties can be expected to be affected by trace metal contaminants.

DYNAMIC LIQUID/SOLID CONTACT ANGLES

TASK IV. THE DYNAMIC CONTACT ANGLE APPARATUS

I. INTRODUCTION

The purpose of the present Task is to develop an experimental apparatus suitable for the measurement of the dynamic contact angle in a solid-liquid-vapor system wherein the liquid moves (relative to the solid) with constant velocity over a dry solid surface. Such an apparatus has been designed and built in this laboratory.

II. APPARATUS

The dynamic contact angle apparatus together with needed accessories is shown in Figure 5. The entire assembly is mounted on a heavy gauge aluminum base plate. The trough is fitted with a wire supply spool with a built-in drag device, a main exterior pulley, a baffle to suppress turbulence, a submerged guide pulley and a wire take-up spool which is indirectly motor driven. The surface of the trough is coated with a film of fluorinated latex to make the test liquid brim over the edge of the trough. The grooved slots underneath the brackets holding the guide pulleys are also coated with the same latex film to prevent test liquid from leaking out via cappillaries formed by the metal-to-metal junctions.

The drag device on the supply spool has thin (approximately 0.005 inch) Teflon discs as bearing surfaces and an adjustable tension spring to allow for a range of tensions under which the wire may be drawn. Attached to the main exterior guide pulley is a set of gears and the smallest, which is in the field of view of the camera, rotates precisely four times faster than the pulley. The smallest gear is marked with numerals 0 to 9 and serves as an event marker in the calculation of wire speed from the motion picture film. The baffle has a portion of its side-wall extend above the liquid level to damp surface turbulence and has a bottom hole about twice the wire diameter to damp vortex formation in the region of the wire/liquid interface. The submerged guide pulley has a Teflon bearing surface and acts with

the main exterior guide pulley to guide the wire perpendicularly through the liquid surface. The take-up spool is driven by a one-half horsepower variable speed motor through two sets of pulleys and a speed reducing gear box. The drive motor has a maximum speed of 10,000 revolutions per minute. A set of pulley combinations is provided for the take-up spool and the gear box output shafts to permit operation of the apparatus at five different wire-speed ranges. The wire speed is controlled for each range by a variable power transformer connected to the variable speed motor drive.

Two high intensity spot lamps were used to illuminate the indicator gear and the wire/liquid interface. A variable shutter motion picture camera operating at 64 frames per second was used to photograph the indicator gear and the wire/liquid interface.

The apparatus was installed in a dry box, fabricated from Plexiglas, in a constant temperature room. The dry box is fitted with a dry air supply, an air recirculation system supplied with 13X molecular sieve as drying agent and a tray of indicating desiccant. It is also provided with two rubber-dam portholes for the camera and for manual adjustments of various components of the apparatus prior to an experimental run.

III. PROCEDURE

The wire is cleaned, dried and tightly wound on a supply spool and threaded through the apparatus to the take-up spool. The apparatus, the lamps and the test liquid are all placed inside the dry box and the trough is filled with the test liquid to brimming. The lens of the movie camera is inserted into the box through an air-tight rubber dam covered port, the lamps are turned on, and the camera focused on the plane which gives sharp images of the wire/liquid interface and the indicator gear. The dry box is flushed with dry air for an hour with the air recirculation system turned on. Air recirculation was maintained throughout the experiment.

A motion picture of the wire moving at constant speed is taken at the solid/liquid interface with the film speed set at 64 frames per second on the camera.

A. Measurement of Contact Angles

Contact angles were measured on a flat ground glass screen from the projected image of a developed film frame using a precision machinists protractor. The set-up consisted of a 35 mm slide projector and a flat mirror to reflect the image to the ground glass screen. Repeatability of measurement is approximately $\pm 3°$. Figure 6 shows a camera view of the solid/liquid interface.

B. Wire Velocity Determination

The wire velocity is calculated from the known circumference of the main exterior guide pulley (30.88 cm), ratio of rotational speeds of pulley and indicator gear (4:1), film speed S, and the number of frames F subtended per revolution of the indicator gear. Thus:

$$V = 30.88 \times \frac{1}{4} \times \frac{S}{F}$$

where V is the wire velocity in cm/sec. Error in measured velocity is estimated to be within $\pm 5\%$ at velocities in the vicinity of 70 cm/sec. In the vicinity of 1 cm/sec, it is estimated to be less than $\pm$ 1%.

TASK V

I. INTRODUCTION

The objective of this phase of the work is the formulation of a mathematical relationship relating the dynamic contact angle to the velocity and necessary properties of the solid, liquid and vapor so that dynamic contact angle can be calculated without resort to experimentation.

To attain this objective, a series of seven liquids in suitable combinations (zero static contact angle) with five solids were investigated. The liquids were absolute alcohol, hexane, iso-propanol, Freon-TF, hexadecane benzyl alcohol and diethyl phthalate. The solids were Type 347 stainless steel, ASTM B 265-58T Grade 6 titanium alloy, Type 6061T6 aluminum alloy, nylon and poly(methyl methacrylate) 20 mil wires. The selected combinations together with the properties of the liquids are given in Table III.

II. EXPERIMENTAL

A. Wire Cleaning Procedure

Titanium wire was degreased with toluene at ambient temperature for 5 minutes, followed by alkaline soaking for 20 minutes at 180°F (Alkon at concentration of 52.5 g/liter). It was then passivated with 30% (by volume) HNO_3 containing 4 oz/gal of potassium dichromate, rinsed thoroughly with distilled water followed by iso-propanol and then dried and wound on a spool[2].

Nylon was washed with Tide detergent, rinsed thoroughly with tap and distilled water. It was then dried and wound on a spool.

Aluminum was degreased with trichloroethylene at ambient temperature, followed by an alkaline bath treatment (CeeBee MX 39 at concentration of 3.7 oz/gal) for 20 minutes at 180°F. It was then rinsed with distilled water followed by iso-propanol, dried and then wound on a spool[2].

The poly(methyl methacrylate) monofilament was specially ordered for this work and required no cleaning prior to use.

The cleaning procedure for stainless steel wire was the same as that for aluminum (2).

B. Contact Angle Measurement

The procedure for filming the solid/liquid interfaces of the different systems studied was essentially the same as that for the model test liquid (absolute alcohol) discussed in the previous Task. Here, however, it was found convenient to do the experiment for a series of solids in combination with one liquid. Thus, a series of experiments may involve Freon TF in combination with any three or all of the five solids. This procedure was accomplished readily by providing each wire with a supply and a take-up spool. A spool of clean wire of ample length may be used for all the test liquids without danger of contamination.

Because of their high viscosities and surface tensions, glycerine and ethylene glycol were among the liquids initially chosen to provide a range of physical properties for the correlation of the dynamic contact angle with the relative velocity of the liquid and solid phases. They were, however, deleted from the list as their dynamic contact angles exceeded 90° even at the low wire velocity limit of the apparatus.

III. RESULTS AND DISCUSSION

The results of the dynamic contact angle measurement for the different systems studied are summarized in Tables IV-X.

Figures 7-11 show the variation of dynamic contact angle with relative velocity of different liquids on a solid substrate. Figures 12-18 show the variation of dynamic contact angle with relative velocity of a liquid on different solid substrates.

The correlations between the physical properties of the liquids and the dynamic contact angle becomes apparent on comparison of these two sets of

figures. It is clear from Figures 11-17 that the effect of the solid substrates on the dynamic contact angle of a wetting liquid (zero static contact angle) is small. Although the effect is small, it is real and significant especially in the low velocity range. The static contact angle of a liquid on a solid surface involves specific interaction between the solid and liquid, and hence depends on the properties of both. It is reasonable to assume that the same specific interaction is still operative when the liquid and the solid are in relative motion.

The physical properties of the liquids, such as viscosity and surface tension, appear to be the predominant controlling factors in the variation of the dynamic contact angle with velocity. In general, the larger the surface tension and viscosity, the larger is the dynamic contact angle of a given liquid at any given velocity.

The dynamic contact angle-velocity curves vary in a predictable manner in terms of the viscosity η and surface tension γ of the liquid, more precisely, in terms of the ratio η/γ. Reference to Table III and Figures 7-11 show that these curves fan towards lower velocities and approach 90° much faster as η/γ increases.

Several equations, including the theoretical expression of Friz[8], were tried in the search for a general functional relation between dynamic contact angle and relative velocity. The experimental data of individual liquid-solid systems were found to fit nicely to an equation of the form:

$$\theta = A \tanh CV + D\sqrt[3]{V}$$

where θ is the dynamic contact angle at velocity V and A, C and D are coefficients. These coefficients must be functions of the properties of the liquid and solid. However, the precise functional relationship has not yet been established.

Table XI shows the computer generated values of these coefficients for the selected liquid-solid system studied. Further work is needed to establish the relationships between these coefficients and the properties of the liquid-solid combinations.

IV. CONCLUSIONS

The results of this phase of the work amply demonstrate, that for solid-liquid systems where the static contact angle is zero, the liquid rather than the solid has the predominant influence on the dynamic liquid-solid contact angle. The solid has, nevertheless, a finite and measurable effect which becomes more significant and apparent at low relative velocities.

BIBLIOGRAPHY

1. A. M. Schwartz, A. H. Ellison, J. D. Galligan and C. A. Rader, NASA Report No. CR 72269.

2. A. M. Schwartz and A. H. Ellison, NASA Report No. CR-54708 of Contract NAS 3-7104, January 13, 1966.

3. G. A. Lyerly and H. Peper, NASA Report No. CR-54175 of Contract NAS 3-5744, December 21, 1964.

4. A. H. Ellison, J. Phys. Chem. 66, 1867 (1962).

5. F. D. Snell and C. T. Snell, "Colorimetric Methods of Analysis", 3rd ed., D. Van Nostrand Company, Incorporated, New York, 1949.

6. S. Sugden, "The Parachor and Valency", George Routledge and Sons, Ltd., London, England (1930), pp. 208-212.

7. R. C. L. Bosworth, Trans. Faraday Soc., 34, 1501 (1938).

8. G. Friz, Z. angew. Physik, 19, 374 (1965).

APPENDIX I

MATERIALS

	Tasks				
	I	II	III	IV	V
Mercury, triple distilled	X	X	X		
Water, double distilled	X	X	X		
Nitric Acid, reagent grade, Fisher Scientific Company	X	X	X		
Zinc, Fisher Scientific Company, sticks	X	X			
Silver, American Smelting and Refining Company, pellets			X		
Copper, Fisher Scientific Company, wire			X		
Lead, Fisher Scientific Company, #8 shot		X			
Bismuth, Fisher Scientific Company, pellets			X		
Tin, Fisher Scientific Company, foil			X		
Nickel, J. T. Baker Chemical Company			X		
Rubidium, K & K Laboratories, Incorporated			X		
Stainless Steel Wire Type 347				X	X
Aluminum Wire, Type 6061T6 alloy					X
Titanium wire, ASTM B 265-58T Grade 6 alloy					X
Poly(methyl methacrylate) monofilament, specially drawn by Fabrics Research Laboratories, Dedham, Massachusetts					X
Nylon monofilament, The Vectra Company					X
Freon TF, duPont fluorocarbon solvent					X
Absolute Alcohol, U. S. Industrial Chemical				X	X
Diethyl phthalate, Fisher Scientific Company					X
Iso-propyl alcohol, Fisher Scientific Company					X
Benzyl alcohol, Matheson, Coleman and Bell					X
Hexane, Fisher Scientific Company					X
Hexadecane, Eastman Kodak, Practical grade					X
Trichloroethylene, Fisher Scientific Company				X	X
Zepel B, fluorinated latex				X	X
Diphenylthiocarbazone (dithizone), Fisher Scientific Company	X	X	X		

APPENDIX II

ANALYTICAL METHODS

A. Dithizone Method

This method of analysis is based on the formation of water-insoluble colored complexes of some metal ions with dithizone (diphenylthiocarbazone). The stabilities of these metal dithizonates in aqueous solution are sensitive to changes in the pH of the solution. Thus by proper, pH control, the different metal dithizonates can be selectively extracted with a suitable organic solvent such as chloroform or carbon tetrachloride. Since the metal dithizonate is colored, the concentration of the metal can be easily determined by comparison of the color intensity of the sample extract with a set of carefully prepared standards. The comparison is conveniently done if a suitable colorimeter or spectrophotometer is available.

B. X-ray and Electron Diffraction Analyses

These methods of analyses are two of the most definitive in determining the chemical nature of the sample, that is, the crystallographic structure of the constituent compounds. The methods depend on the scattering of X-ray or high energy electron beams by a crystalline material which acts as a three-dimensional grating in the same manner as light waves are diffracted by gratings with closely spaced lines with spacings of the order of magnitude of the wavelength of light.

The diffraction pattern, reflects the internal geometry of the crystal and maybe used to identify unambiguously the kind and crystalline form of the material. For single crystals, the diffraction pattern occurs as spots, but for materials in random orientation such as a crystalline powder, the diffraction pattern appears as rings on a photographic film or plate, due to partial destructive interference of the diffracted beams. Positive identification of the crystalline form of the sample is usually done by pattern matching with a known standard. The analysis of our sample were done for us by an outside laboratory.

C. Polarography

This method of analysis is based upon the determination of current flow when a solution containing an oxidizable or reducible substance is electrolyzed in a cell in which one electrode consists of mercury dropping from a fine-bore capillary. As the potential is increased from zero, the current flowing through the solution remains small until one of the component begins to be reduced at the mercury cathode. The reduction process is accompanied by a rapid rise in current. The current increase is a function of the concentration of the material and the applied potential corresponding to one half the current rise is characteristic of the material being reduced. Thus quantitative as well as qualitative analyses of a sample is possible with this method. Polarographic analysis of the surface films were performed using a Fisher Electropode Model 65.

TABLE I

ANALYSIS OF SURFACE FILMS ON
CONTAMINATED MERCURY

	Method			
Contaminant	Dithizone	Polarography	X-ray	Electron Diffraction
None	Hg^{++} (5.4%)	Pb (trace)	Amorphous	—
Zn	Hg^{++} (0.7%) Zn (61%)	—	ZnO	ZnO
Pb	Hg^{++} (2.5%) Pb (96%)	—	PbO	PbO
Bi	Hg^{++} (1.5%)	Bi (8.7%)	Amorphous	—
Cu	Hg^{++} (3.5%)	Cu (4.7%)	Amorphous	—
Sn	Hg^{++} (2.5%)	Sn (12%)	Amorphous	—
Rb	Surface film could not be isolated by the technique developed.			

TABLE II

APPARENT EQUILIBRIUM SURFACE POTENTIAL OF MERCURY CONTAINING 2 PPM SOLUBLE CONTAMINANTS

Contaminants	Potentials (volts)
None	-0.185
Pb[a]	+0.500
Zn[a]	+0.230
Cu	-0.145
Sn	-0.492
Bi	-0.440
Ag	-0.250
Rb	-0.525

a. Values estimated from Reference (1).

TABLE III

SOLID-LIQUID SYSTEMS FOR DYNAMIC CONTACT ANGLE MEASUREMENTS

Liquid	Density (°C) (grams/ml)	Viscosity (°C) (centipoise)	Surface Tension (°C) (dynes/cm)	Stainless Steel	Titanium	Aluminum	Nylon	Poly(methyl methacrylate)
Absolute Alcohol	0.7893^{20} [a]	1.200^{20} [a]	22.75^{20} [a]	X	X		X	
Freon TF	1.5700^{21} [b]	0.694^{21} [b]	19.00^{25} [b]	X	X		X	
Hexane	0.6603^{20} [a]	0.326^{20} [a]	18.43^{20} [a]	X		X	X	X
Iso-propanol	0.7854^{20} [a]	2.220^{22} [a]	21.70^{20} [a]	X	X		X	
Hexadecane	0.7751^{20} [a]	3.320^{20} [a]	27.60^{20} [c]	X	X	X	X	X
Benzyl Alcohol	1.0500^{15} [a]	5.800^{20} [a]	39.00^{20} [a]	X		X	X	X
Diethyl phthalate	1.1230^{25} [a]	10.100^{25} [d]	37.50^{20} [a]	X	X	X		

a. Handbook of Chemistry and Physics, Chemical Rubber Publishing Company, 44th ed.

b. du Pont Technical Bulletin.

c. A.I.J. Vogel, J. Chem. Soc. (London) 133 (1946).

d. International Critical Tables, Vol. VII. p. 211.

TABLE IV

DYNAMIC CONTACT ANGLE-VELOCITY DATA FOR SOLIDS/ABSOLUTE ALCOHOL SYSTEMS

Stainless Steel		Titanium		Nylon	
Velocity	Angle	Velocity	Angle	Velocity	Angle
0	0	0	0	0	0
3.75	42	2.86	53	2.93	61
5.80	52	5.56	59	5.56	66
8.02	57	8.18	63	8.41	69
8.99	62	10.34	67	10.81	73
12.7	64	12.97	69	13.58	71
13.25	64	15.67	71	16.13	73
19.1	65	17.83	72	18.45	76
19.1	66	19.92	73	20.69	77
28.7	73	22.47	75	22.47	77
32.3	74	24.63	76	24.63	78
32.3	75	28.72	80	27.25	78
36.8	76	32.35	81	28.72	79
39.7	80			30.42	79
				32.35	79

TABLE V

DYNAMIC CONTACT ANGLE - VELOCITY DATA FOR SOLID/FREON TF SYSTEMS

Stainless Steel		Titanium		Nylon	
Velocity	Angle	Velocity	Angle	Velocity	Angle
0	0	0	0	0	0
1.30	34	1.62	50	1.17	51
2.90	43	3.71	56	3.63	56
4.65	49	5.33	59	5.25	62
6.81	59	6.72	62	6.95	66
8.05	64	7.95	64	8.18	69
8.50	65	9.34	69	9.26	71
8.70	64	13.20	67	9.96	71
15.4	64	14.13	71	12.12	75
35	72	15.75	72	12.43	76
36.7	75	16.37	72	14.59	75
		17.80	72	16.13	78
		18.50	72	17.22	79

TABLE VI

DYNAMIC CONTACT ANGLE-VELOCITY DATA FOR SOLID/HEXANE SYSTEMS

Stainless Steel		Aluminum		Nylon		PMMA[a]	
Velocity	Angle	Velocity	Angle	Velocity	Angle	Velocity	Angle
0	0	0	0	0	0	0	0
3.86	47	1.78	33	3.97	44	2.65	44
6.48	52	6.95	42	7.12	49	8.68	50
11.12	55	8.96	50	11.55	51	12.10	52
14.13	59	12.43	54	18.40	53	17.70	56
17.06	61	13.97	53	21.40	53	20.40	56
21.54	62	14.59	57	22.70	56	30.30	58
25.86	63	18.61	61	29.10	56	32.20	61
32.35	66	20.69	62	31.40	56	35.20	61
34.51	67	23.55	64	34.30	60	39.70	61
43.08	67	25.86	65	36.80	60	47.00	63
57.44	67	32.35	66	37.20	56	57.00	67
64.69	67	39.76	66	48.00	57	62.90	67
		43.08	66	51.50	65	70.90	67
		47.01	66	64.90	70		
		57.44	71				

a. Poly(methyl methacrylate)

TABLE VII

DYNAMIC CONTACT ANGLE-VELOCITY DATA FOR SOLID/ISO-PROPANOL SYSTEMS

Stainless Steel		Titanium		Nylon	
Velocity	Angle	Velocity	Angle	Velocity	Angle
0	0	0	0	0	0
1.87	56	2.06	54	1.43	52
3.46	60	3.60	59	3.36	60
3.97	63	4.95	62	4.25	60
7.18	62	6.30	63	5.55	64
7.18	64	7.72	63	6.75	62
8.00	62	8.50	62	8.33	64
8.51	64	9.95	63	8.50	64
9.30	63	10.50	66	9.08	66
9.95	66	10.75	66	10.50	64
11.00	67	11.50	66	10.70	64
12.05	68	12.00	66	18.50	69
13.60	66	13.30	66		
13.90	69	14.00	66		
15.20	69	16.10	71		
16.20	74	17.30	71		
16.60	74				
22.30	74				

TABLE VIII

DYNAMIC CONTACT ANGLE-VELOCITY DATA FOR SOLID/BENZYL ALCOHOL SYSTEMS

Stainless Steel		Aluminum		Nylon		PMMA[a]	
Velocity	Angle	Velocity	Angle	Velocity	Angle	Velocity	Angle
0	0	0	0	0	0	0	0
0.54	55	0.41	50	0.36	55	0.39	54
0.98	62	0.84	56	0.93	60	0.86	58
1.03	60	1.31	57	1.22	63	1.45	62
1.40	65	1.75	59	1.87	66	1.98	65
1.75	66	2.07	62	2.33	68	2.74	69
1.91	67	2.37	64	2.70	72	3.52	70
2.25	69	2.85	71	3.10	73	3.97	71
2.71	72	3.10	70	3.20	74	4.47	74
2.93	71	3.92	70	3.65	76	4.86	74
3.06	76	4.00	70	4.07	77	5.14	74
3.34	76	4.35	70	4.42	77	5.90	74
4.02	74	5.25	70	4.83	77		
4.15	79	5.55	70	5.32	77		
4.79	77			5.67	77		
5.81	77						

a. Poly(methyl methacrylate)

TABLE IX

DYNAMIC CONTACT ANGLE-VELOCITY DATA FOR SOLID/HEXADECANE SYSTEMS

Stainless Steel		Titanium		Aluminum		Nylon		PMMA[a]	
Velocity	Angle	Velocity	Angle	Velocity	Angle	Velocity	Angle	Velocity	Angle
0	0	0	0	0	0	0	0	0	0
0.82	35	0.99	55	1.19	43	1.05	52	0.51	42
1.97	45	1.30	53	2.05	55	1.88	58	1.04	51
3.02	54	2.07	58	3.16	59	3.02	64	2.47	61
3.85	59	3.07	62	3.78	63	3.66	68	3.07	65
4.77	64	4.00	66	5.01	65	5.14	73	4.21	65
6.40	71	5.10	70	5.44	67	5.90	75	5.42	66
6.48	67	5.25	71	6.46	68	7.12	76	5.93	68
7.72	74	6.51	72	7.90	68	8.70	80	8.31	69
8.60	76	7.72	73	9.10	70	10.2	79	8.93	70
10.45	76	9.08	73	10.80	72	11.2	79	10.30	71
11.70	77	10.20	76	12.00	73	13.60	79	12.90	74
12.90	78	11.70	76	13.20	74	14.80	79	15.20	75
13.60	79	12.30	74	15.20	77	16.20	79	16.10	75
15.20	80	13.20	78	16.80	77	17.90	82	16.70	76
		14.80	78	17.20	81				
		15.70	78	17.80	79				

a. Poly(methyl methacrylate)

TABLE X

DYNAMIC CONTACT ANGLE-VELOCITY DATA FOR SOLID/DIETHYL PHTHALATE SYSTEMS

Stainless Steel		Titanium		Aluminum	
Velocity	Angle	Velocity	Angle	Velocity	Angle
0	0	0	0	0	0
0.26	42	0.40	53	0.31	52
0.41	54	0.57	59	0.52	56
0.74	63	0.79	62	0.73	60
1.26	70	0.80	65	1.28	66
1.46	73	1.23	66	1.80	69
1.76	77	1.43	67	2.17	70
2.21	77	1.65	70	2.64	73
2.57	79	1.75	65	2.83	70
2.98	83	1.98	72	3.05	72
3.35	83	2.05	73	3.31	74
3.80	84	2.31	73	3.42	75
4.15	85	2.48	74	3.86	74
		2.77	80	4.55	75
		3.27	80		
		3.66	84		
		3.70	84		

TABLE XI

VALUES OF COEFFICIENTS FOR BEST THEORETICAL FIT OF EQUATION $\theta = A \tanh CV + D \sqrt[3]{V}$ TO EXPERIMENTAL DYNAMIC CONTACT ANGLE-VELOCITY DATA

	A	C	D
ABSOLUTE ALCOHOL			
Stainless Steel	32.7191	0.223752	13.1107
Titanium	33.3641	0.611684	14.9583
Nylon	50.7405	0.613541	9.2143
FREON-TF			
Stainless Steel	38.9887	0.372942	11.1024
Titanium	39.5	0.75	13
Nylon	40	0.3	15
HEXANE			
Stainless Steel	38.2258	0.35634	8.29626
Aluminum	32	0.2	10.5
Nylon	33.5	0.35	8.5
PMMA	31.5	0.35	9
ISO-PROPANOL			
Stainless Steel	41.8377	1.64541	11.4106
Titanium	44.8054	0.629019	9.46552
Nylon	49.3912	0.983202	7.21221
HEXADECANE			
Stainless Steel	24.7744	0.45414	23.2897
Titanium	42.8792	0.988344	14.3057
Aluminum	40.0281	0.715207	14.5941
Nylon	47.3875	0.864954	13.7545
PMMA	43.4394	1.67898	12.9909

CONTINUED

TABLE XI (Conclusion)

	A	C	D
BENZYL ALCOHOL			
Stainless Steel	40.5217	2.79451	21.8634
Aluminum	34.8306	5.19407	22.123
Nylon	39.2927	7.98417	22.5646
PMMA	40.6481	7.7127	19.2287
DIETHYL-PHTHALATE			
Stainless Steel	40.6584	2.708	28.2268
Aluminum	41.2935	4.63314	21.5271
Titanium	28.8934	5.21322	34.3305

Figure 1. Trough and Barriers for Surface Film Collection.

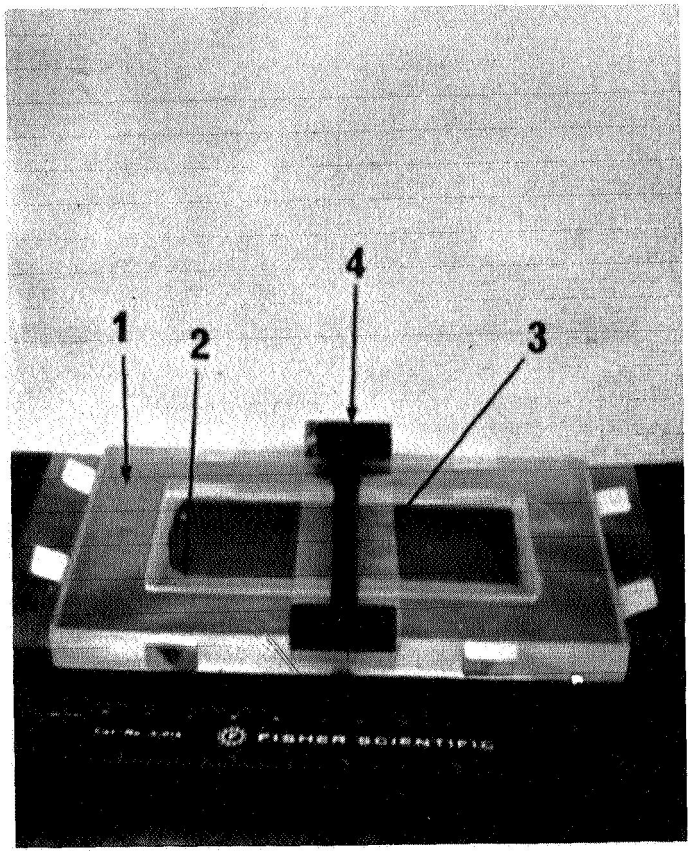

1. Plexiglas trough
2. Fixed Mylar frame
3. Mylar sweeping barrier
4. Brass support

Figure 2. Surface Film on Contaminated Mercury.

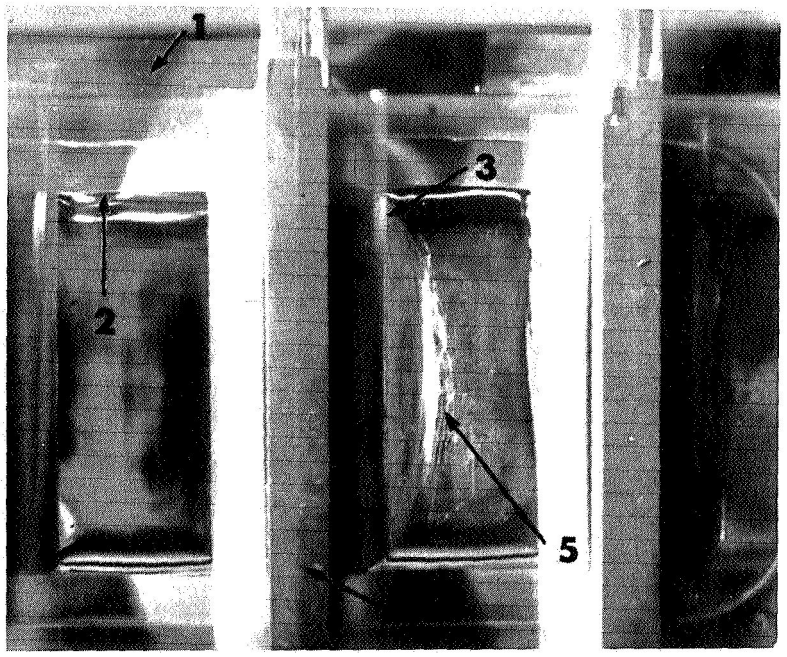

1. Plexiglas trough
2. Fixed Mylar frame
3. Mylar sweeping barrier
4. Brass support
5. Swept surface film

Figure 3. Photomicrograph of Surface Film Collected From Zinc-contaminated Mercury.

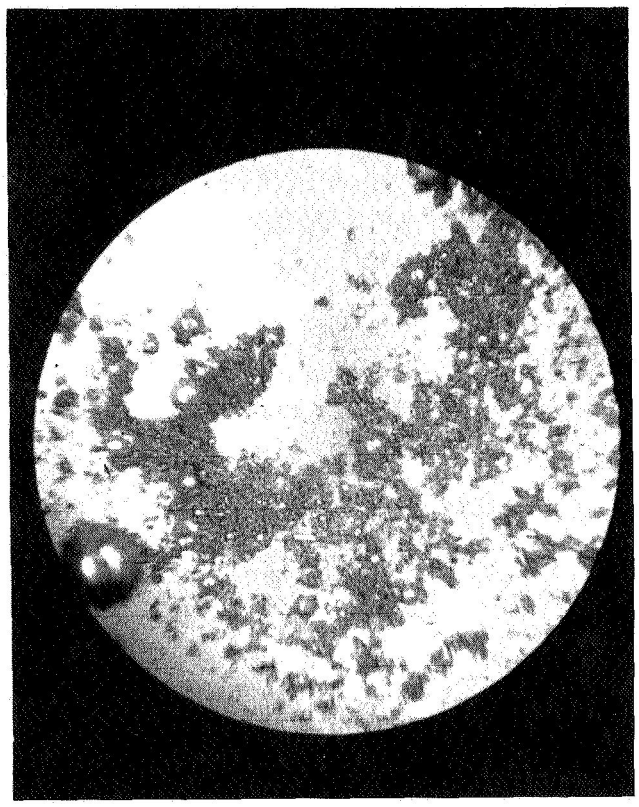

Figure 4. The Maximum Bubble Pressure Apparatus.

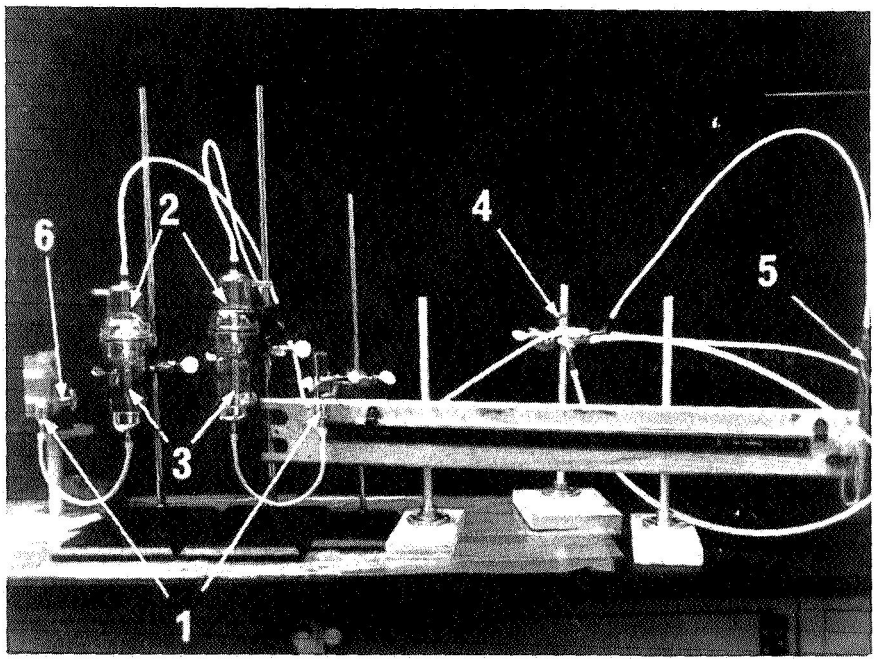

1. Leveling bulb
2. Bubbler housing
3. Capillary jets
4. Needle valve
5. Mercury manometer
6. Screw manipulator

Figure 5. Dynamic Contact Angle Apparatus.

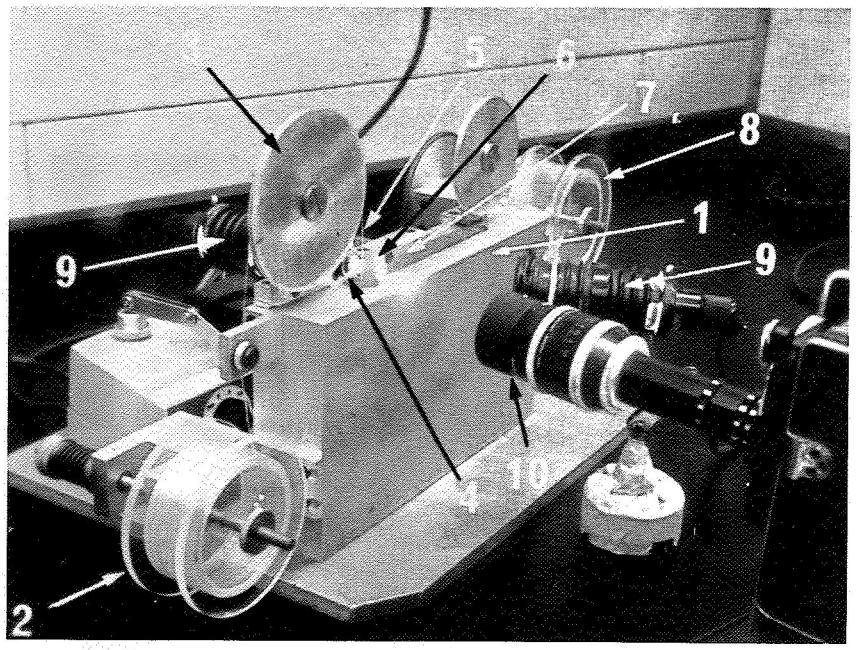

(a)

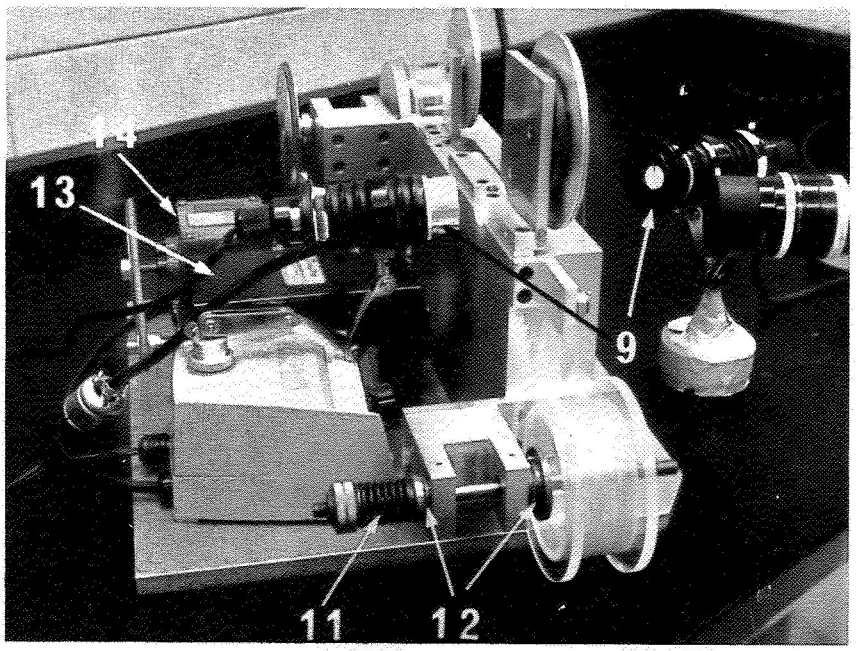

(b)

1. Aluminum trough
2. Supply spool
3. Main exterior guide pulley
4. Indicator gear
5. Wire
6. Baffle
7. Interior guide pulley bracket
8. Take-up spool
9. Spot lamps
10. Camera
11. Tension spring
12. Teflon discs
13. Drive motor
14. Speed reducer

Figure 6. Camera View of Solid/Liquid Interface of Stainless Steel/Absolute Alcohol at (a) Zero and (b) 13.25 cm/sec relative velocity.

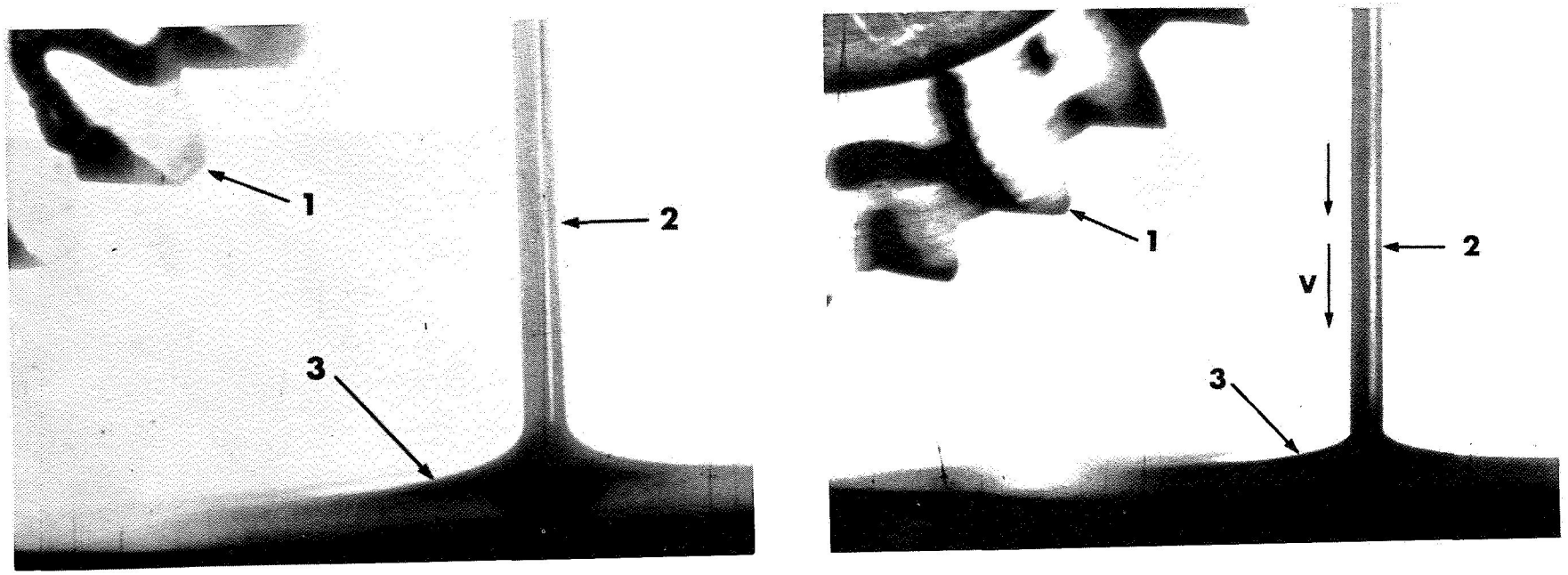

(a) (b)

1. Indicator gear
2. Wire
3. Liquid surface

Figure 7. Variation of Dynamic Contact Angle with Velocity on a Stainless Steel Surface.

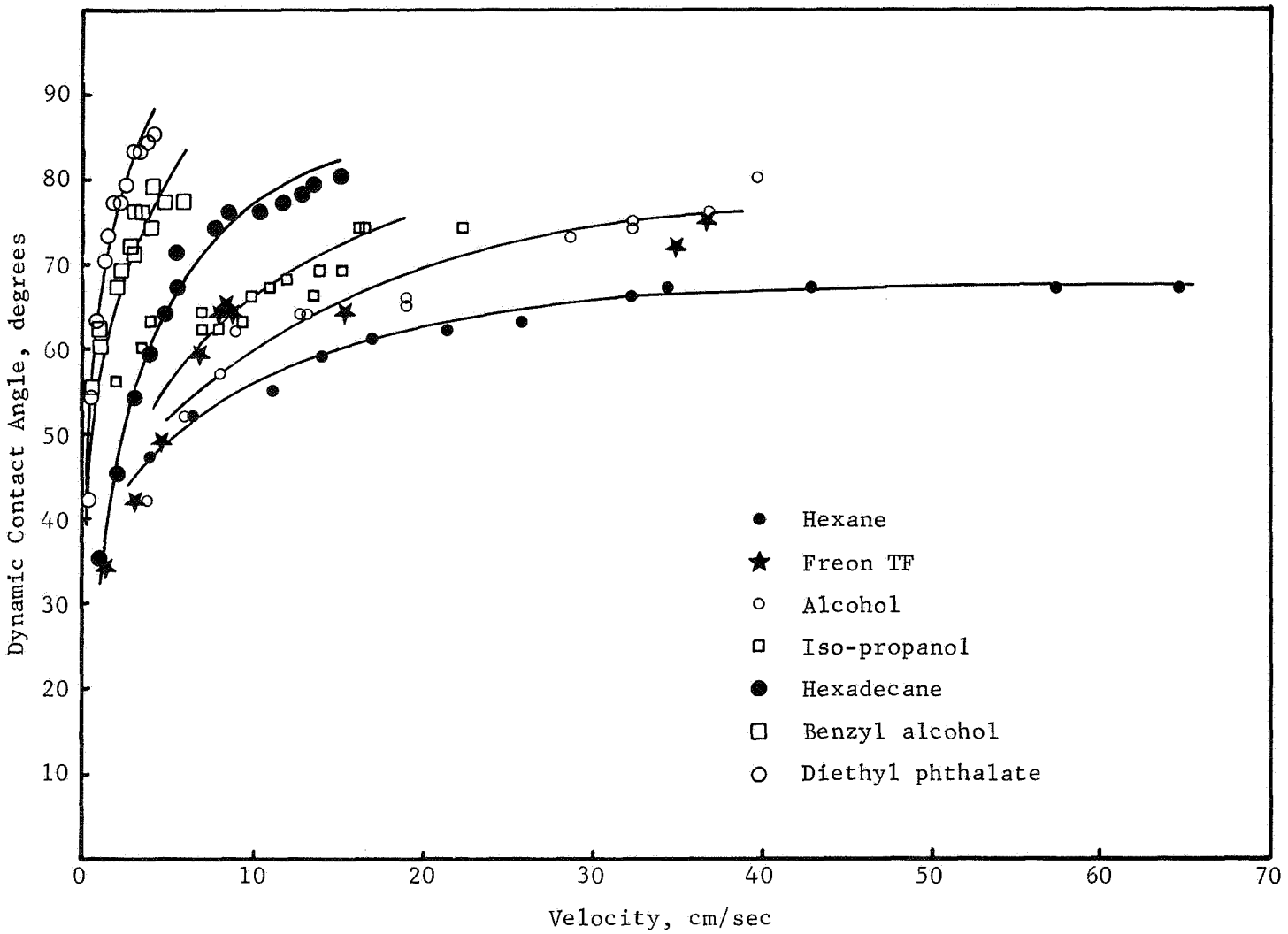

Figure 8. Variation of Dynamic Contact Angle with Velocity on a Titanium Surface.

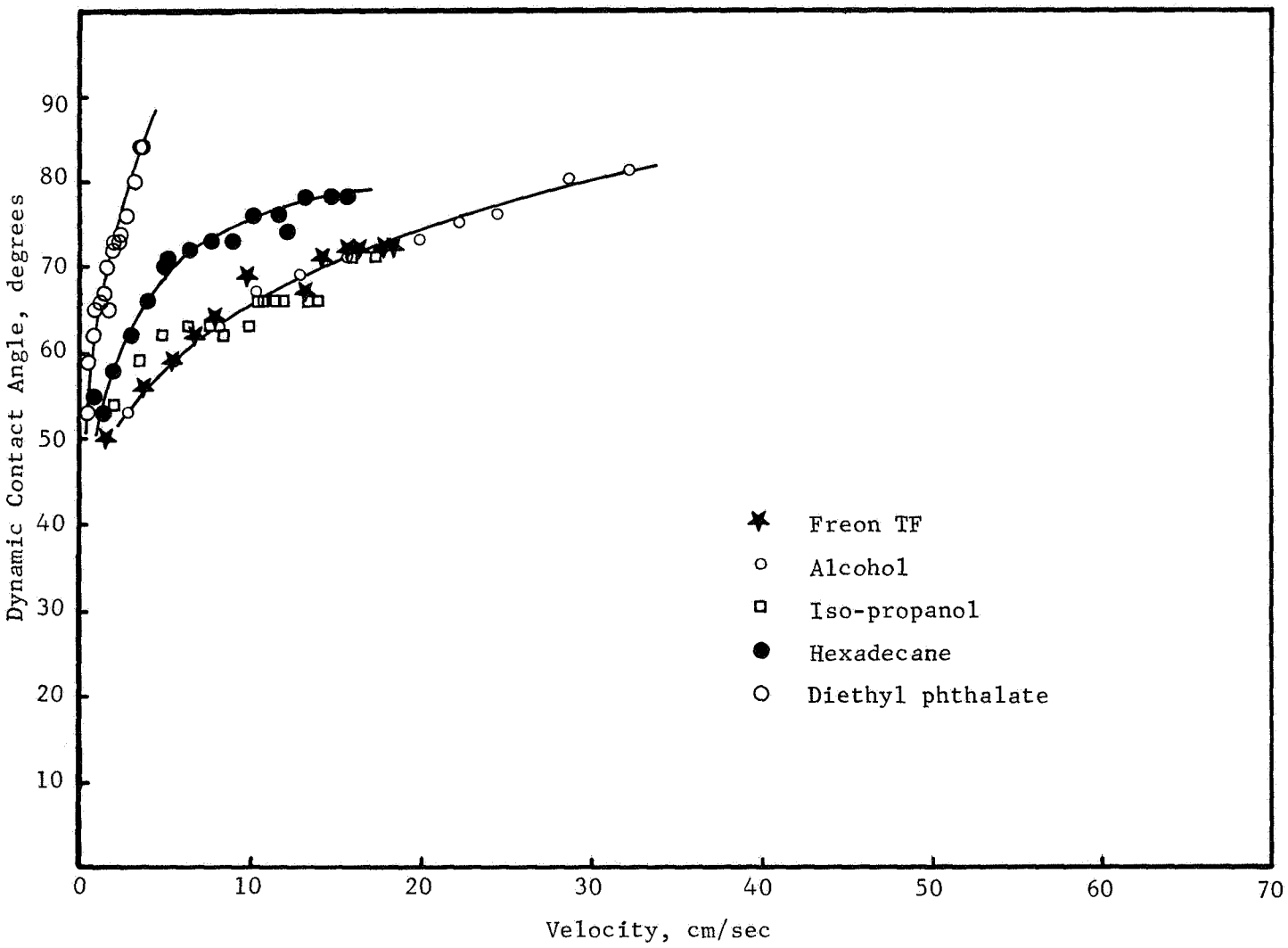

Figure 9. Variation of Dynamic Contact Angle with Velocity on an Aluminum Surface.

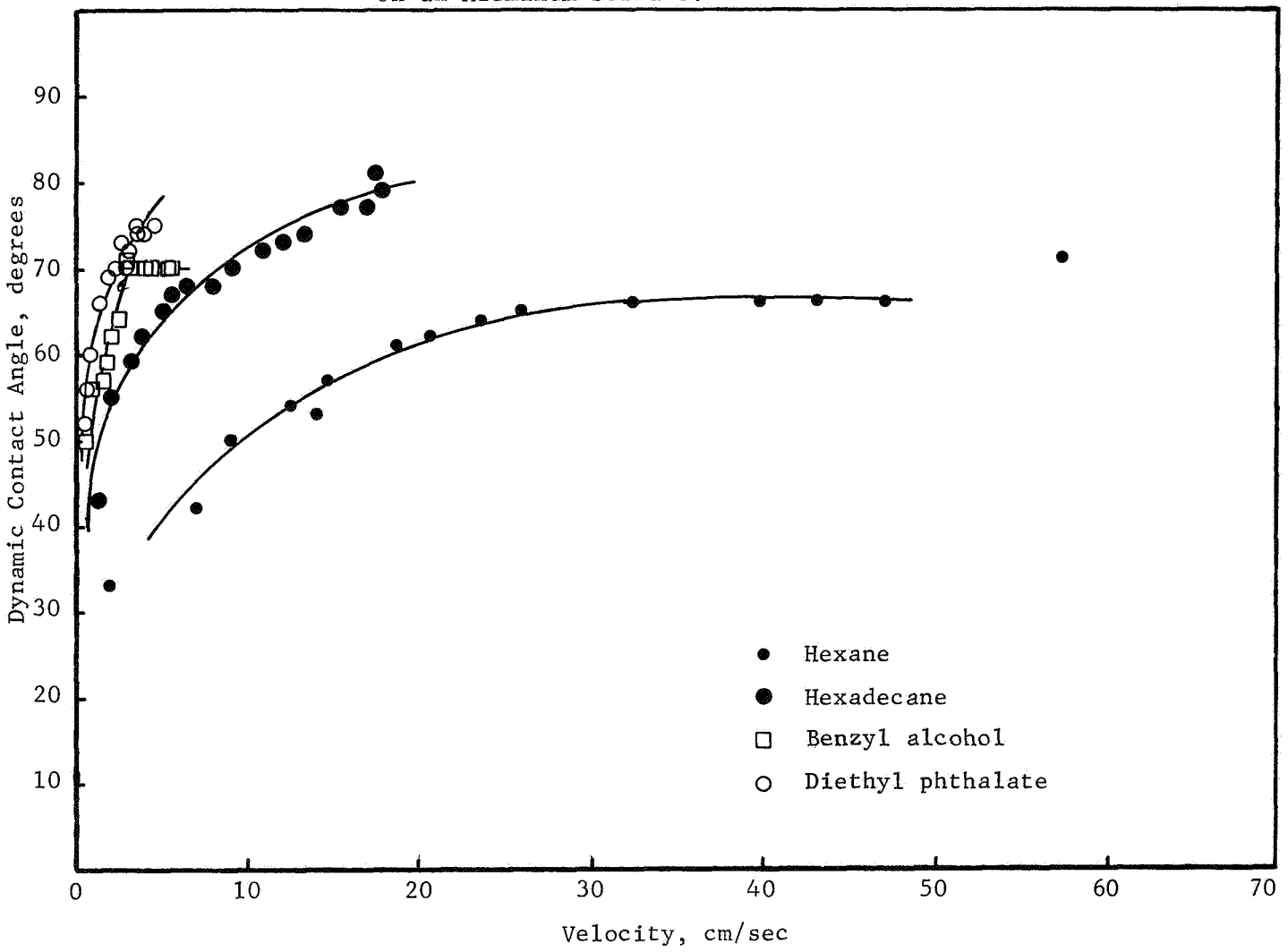

Figure 10. Variation of Dynamic Contact Angle with Velocity on a Nylon Surface.

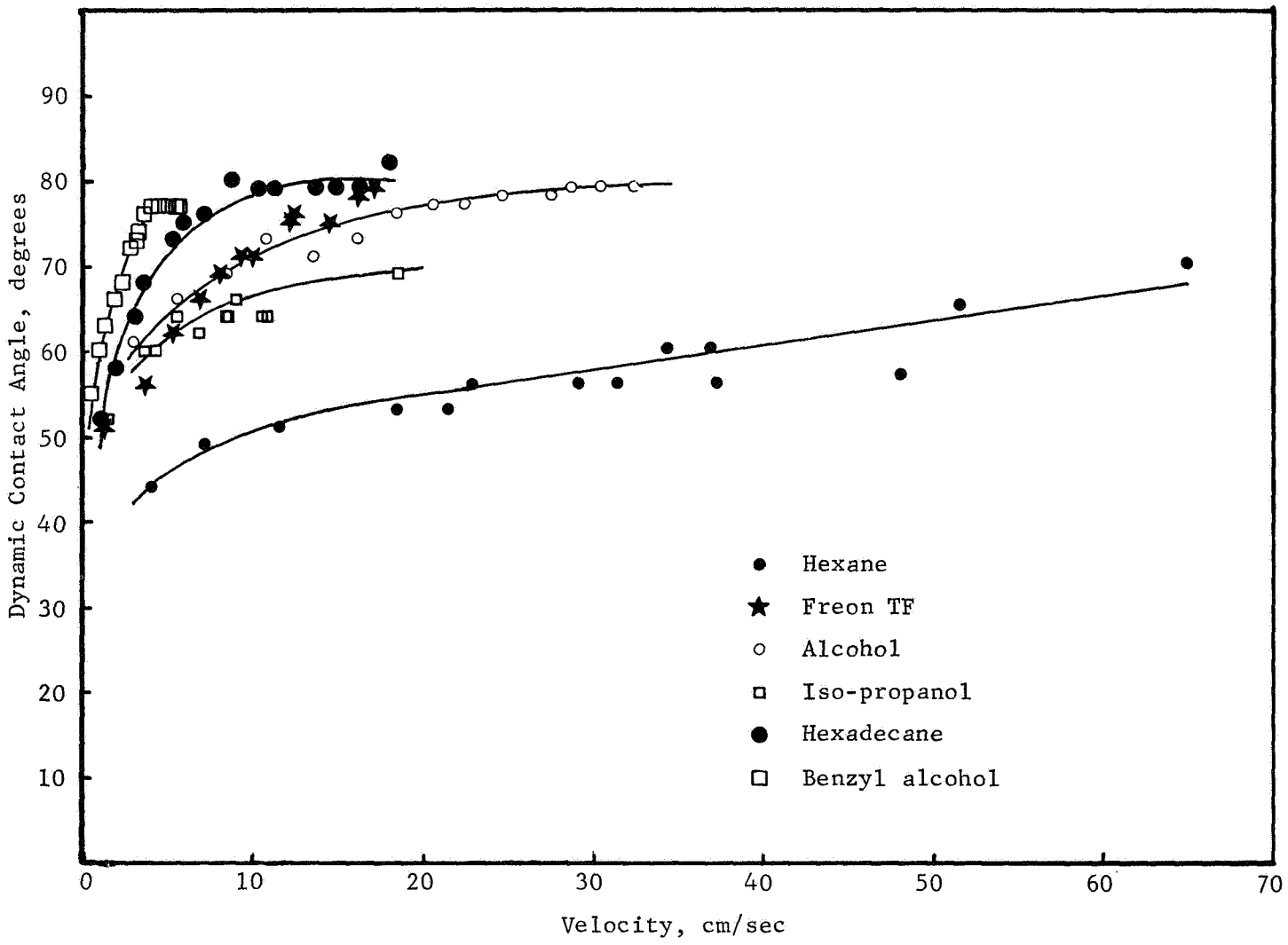

Figure 11. Variation of Dynamic Contact Angle with Velocity on a Poly(methyl methacrylate) Surface.

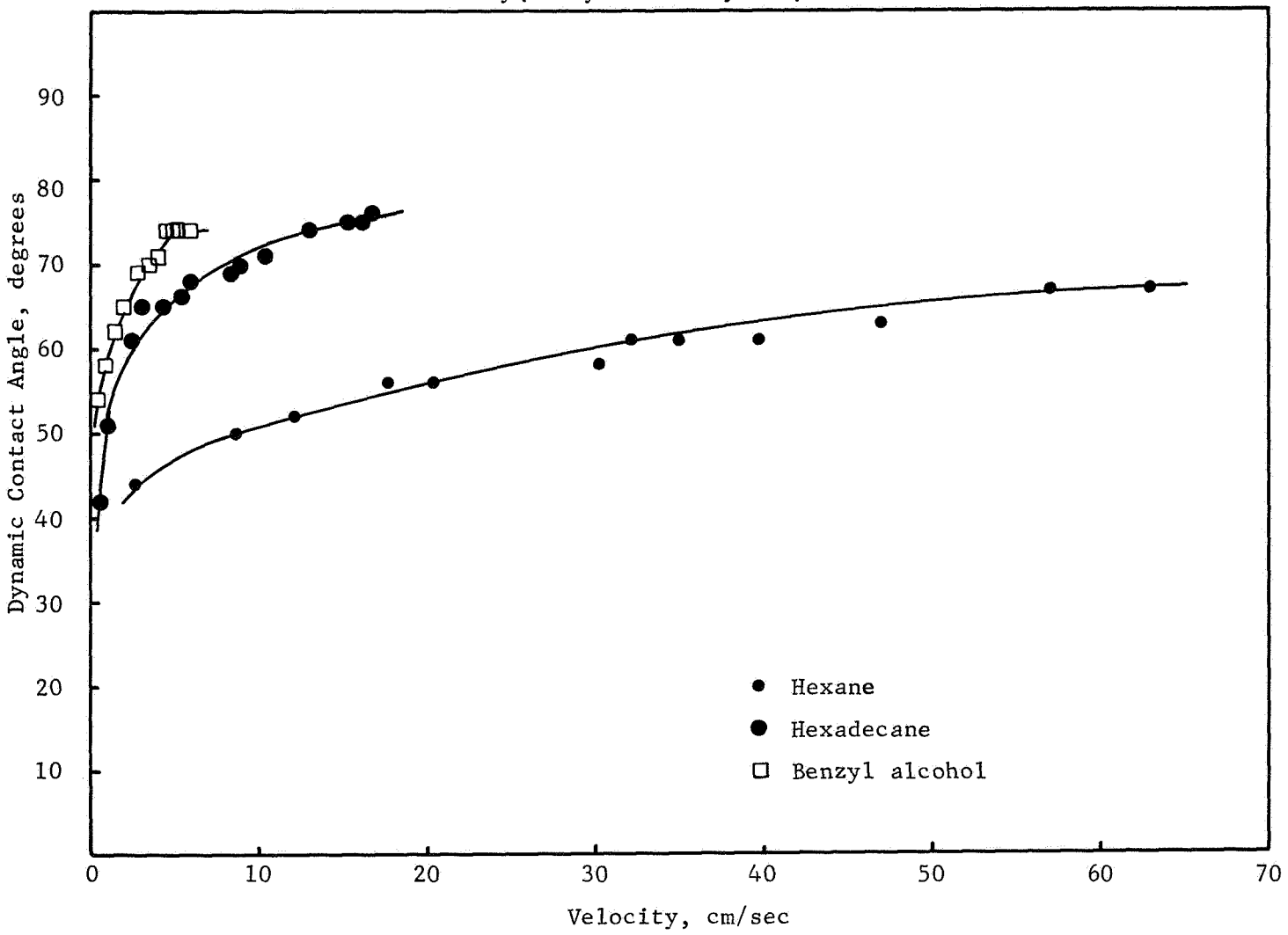

Figure 12. Variation of the Dynamic Contact Angle of Alcohol With Velocity.

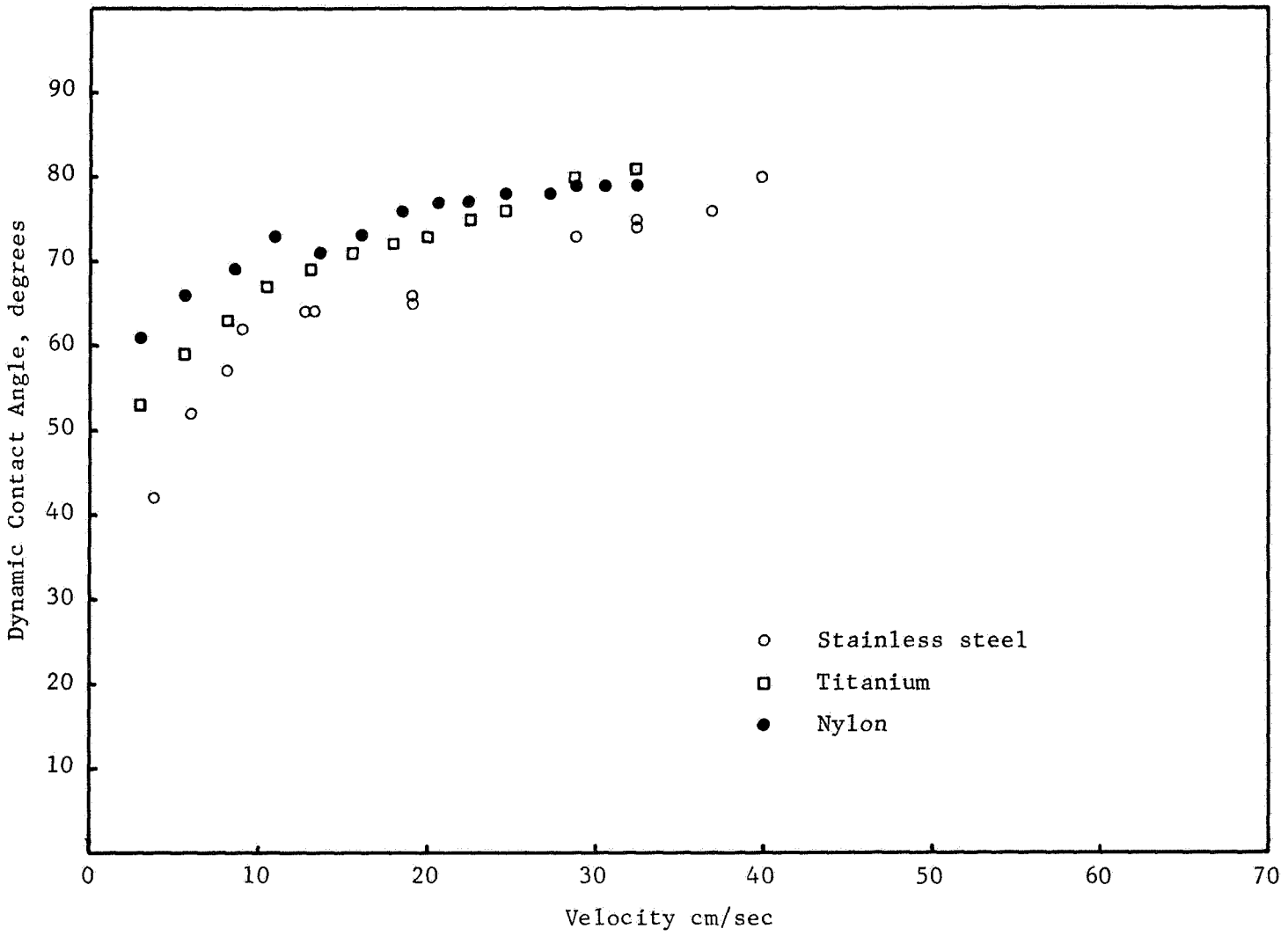

Figure 13. Variation of the Dynamic Contact Angle of Freon TF with Velocity.

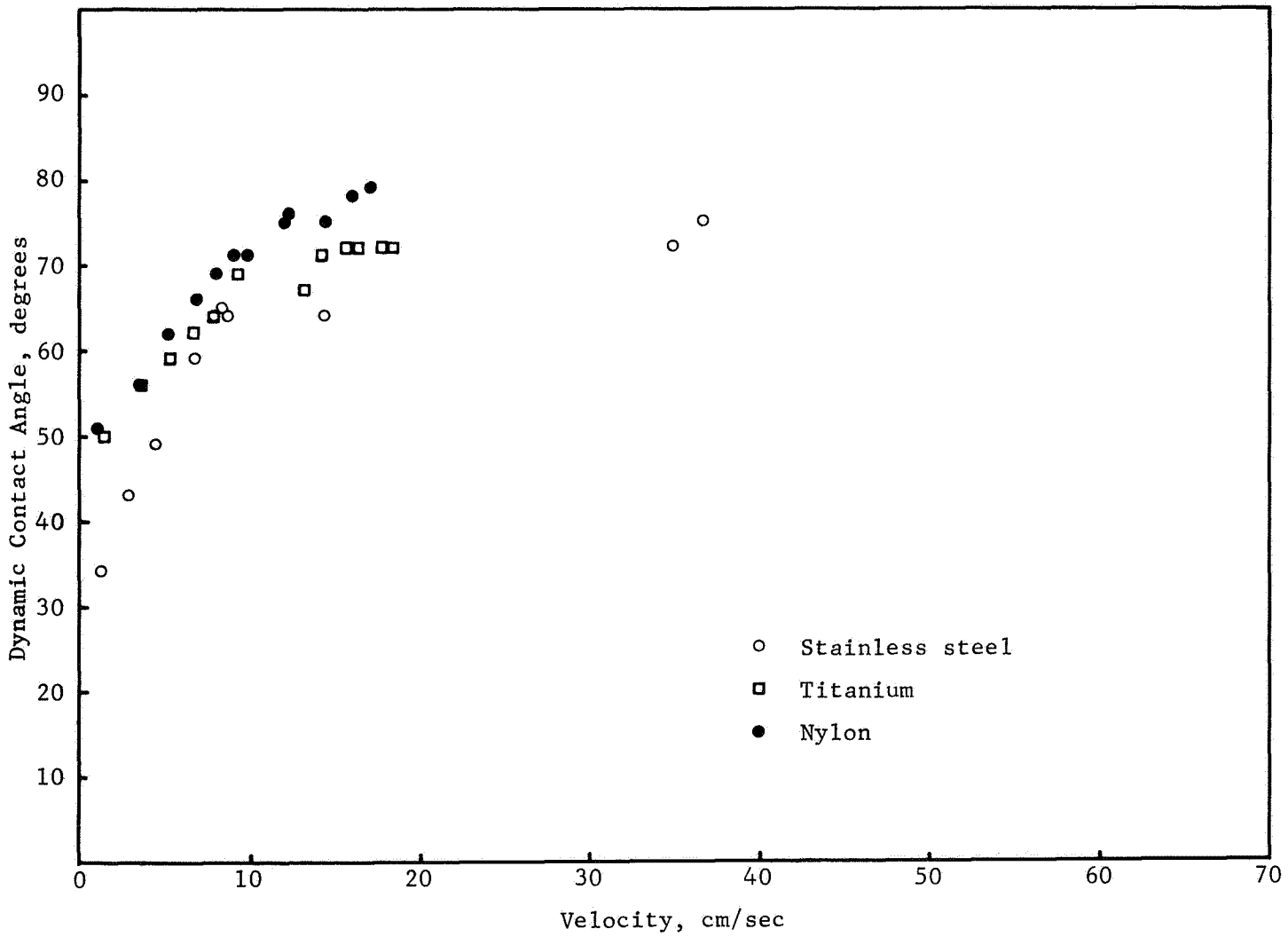

Figure 14. Variation of the Dynamic Contact Angle of Hexane with Velocity.

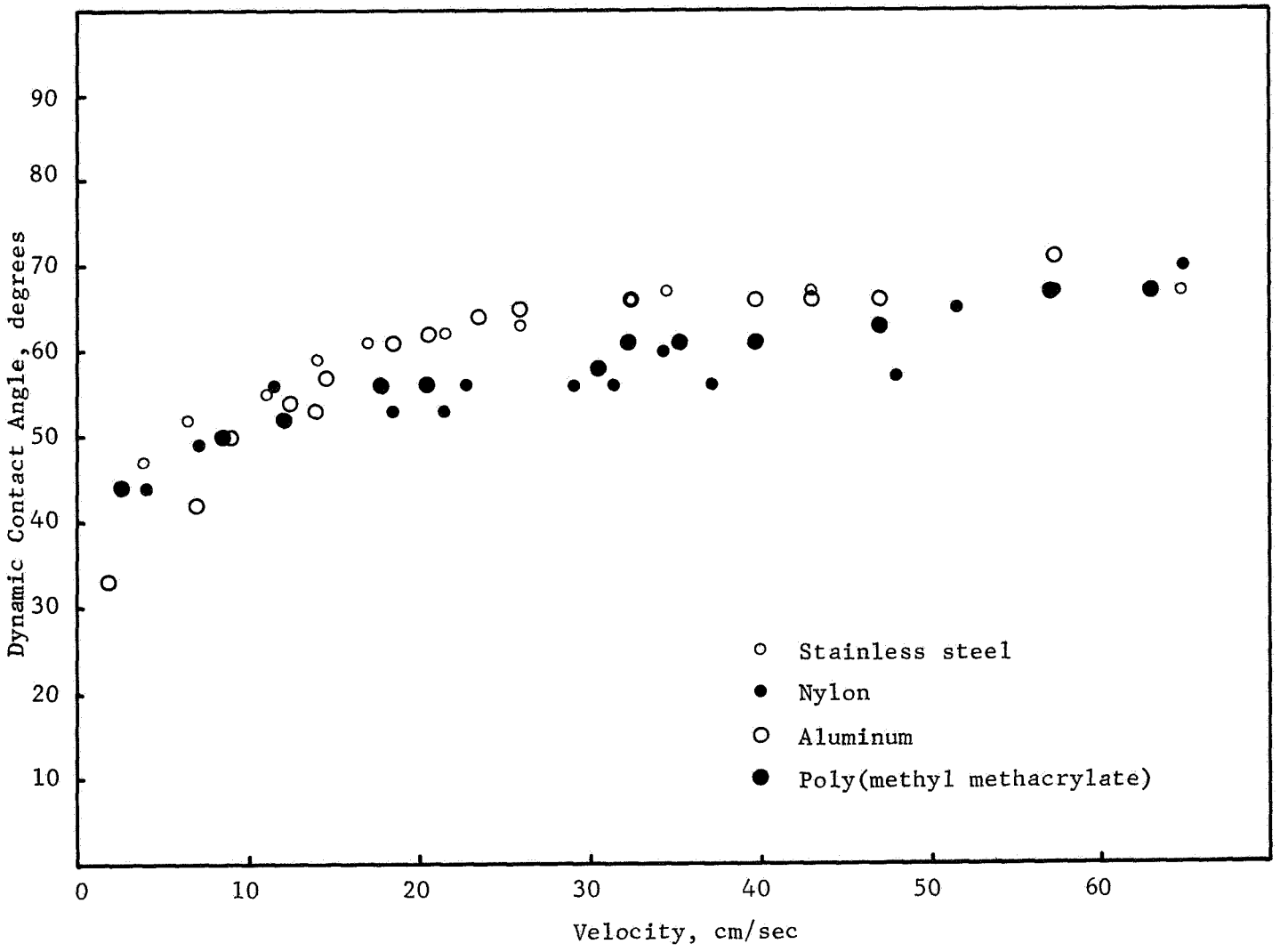

Figure 15. Variation of the Dynamic Contact Angle of Iso-propanol with Velocity.

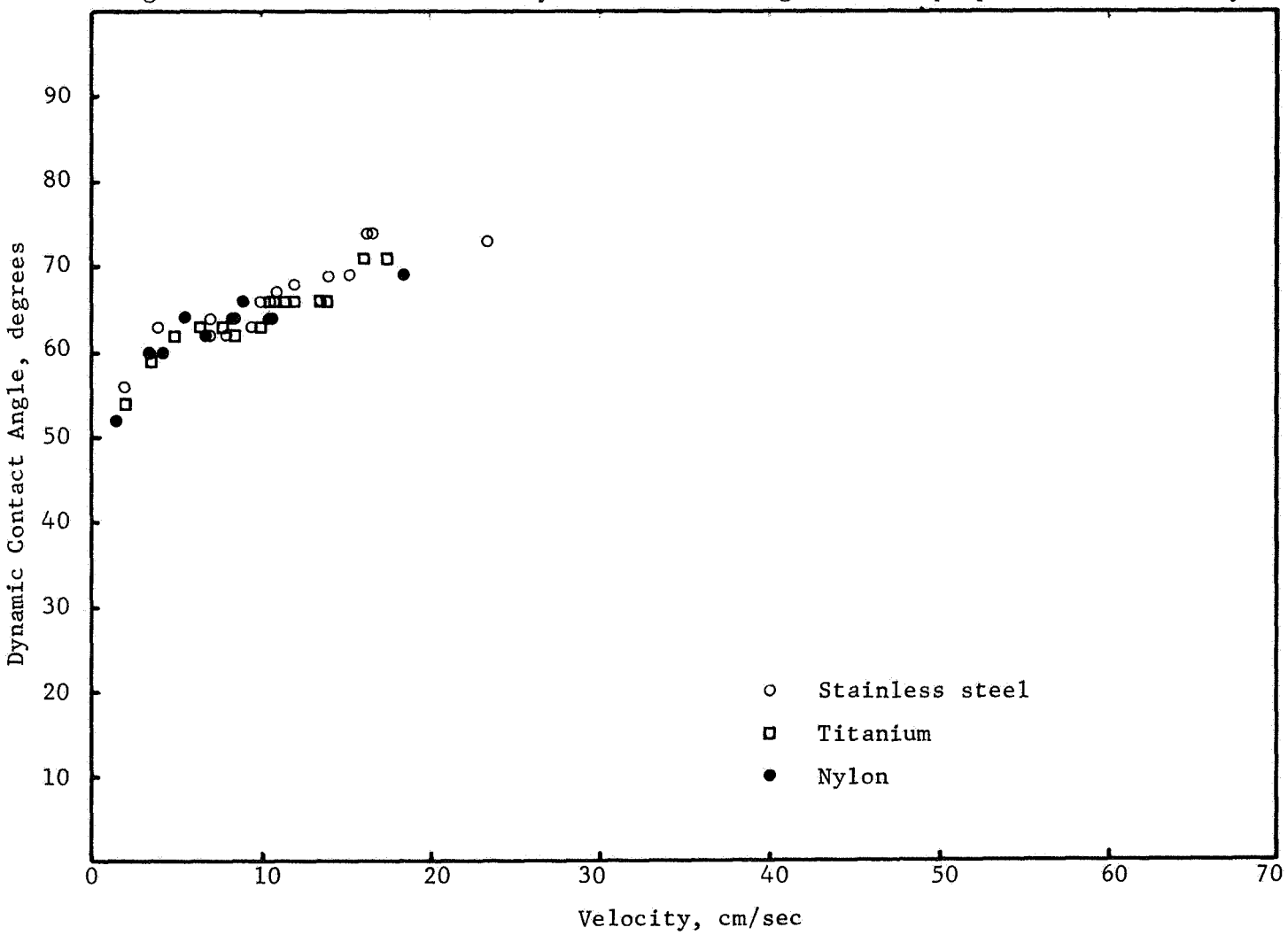

Figure 16. Variation of the Dynamic Contact Angle of Benzyl Alcohol with Velocity.

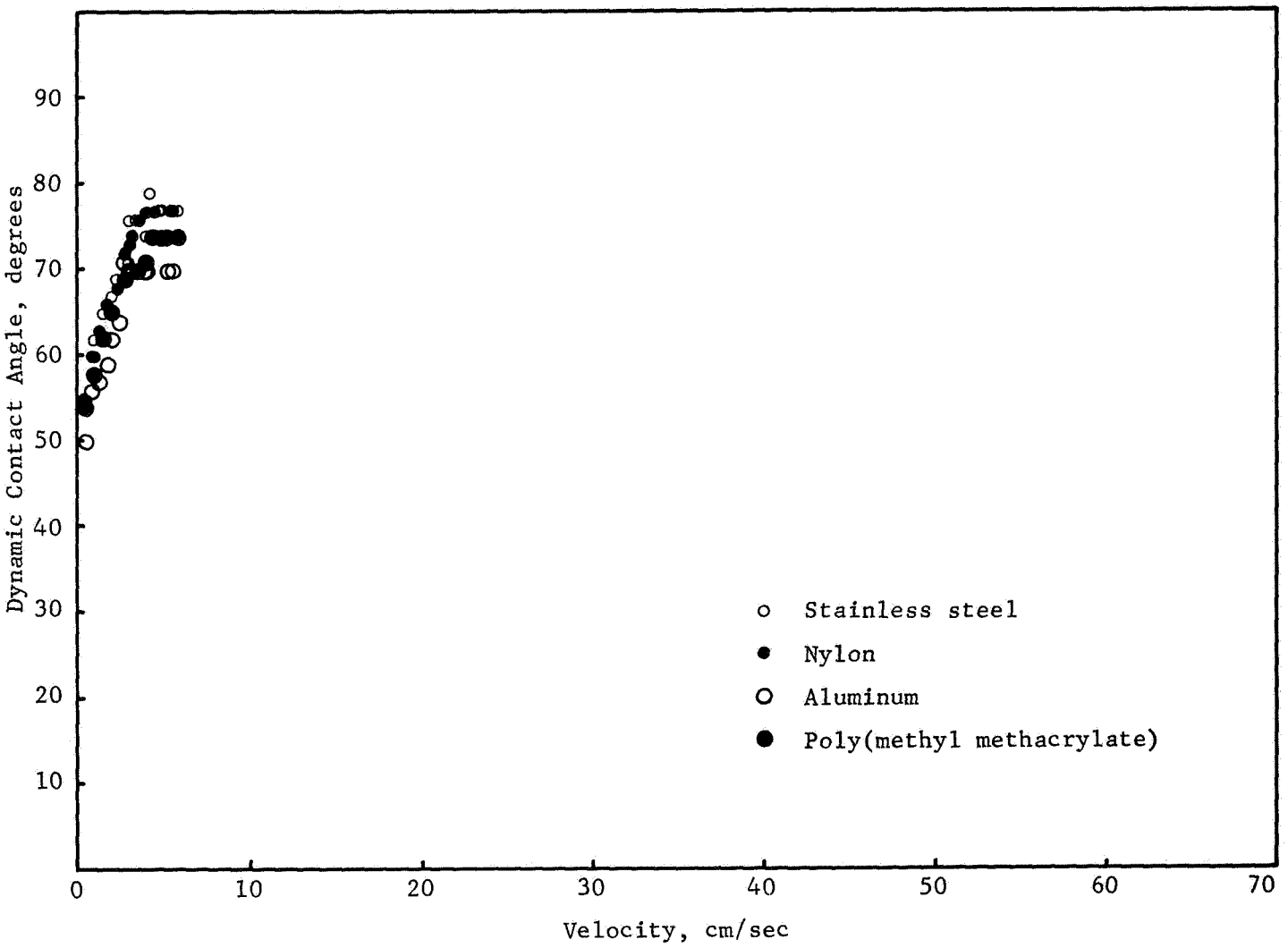

Figure 17. Variation of the Dynamic Contact Angle of Hexadecane with Velocity.

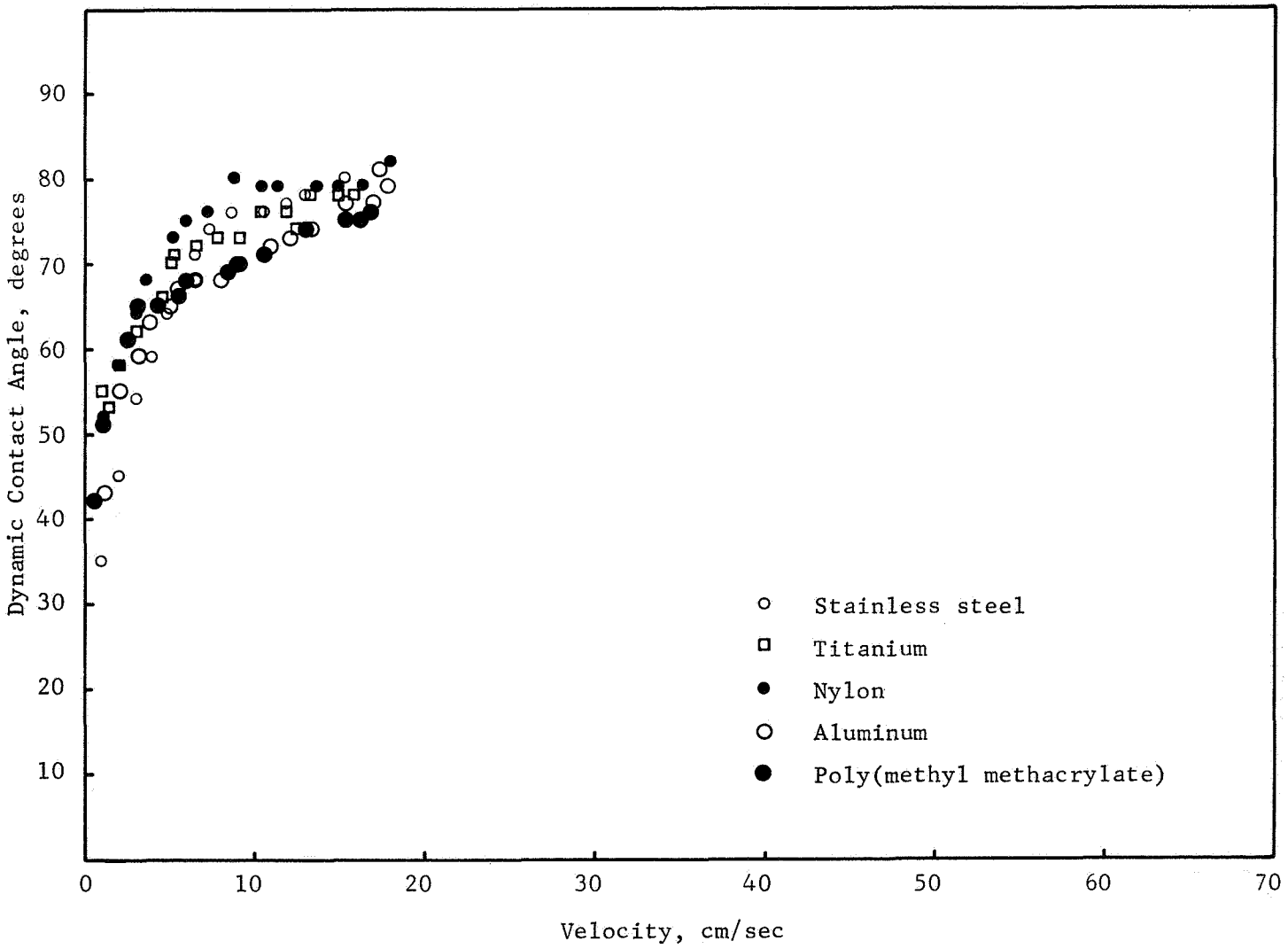

Figure 18. Variation of the Dynamic Contact Angle of Diethyl Phthalate with Velocity.

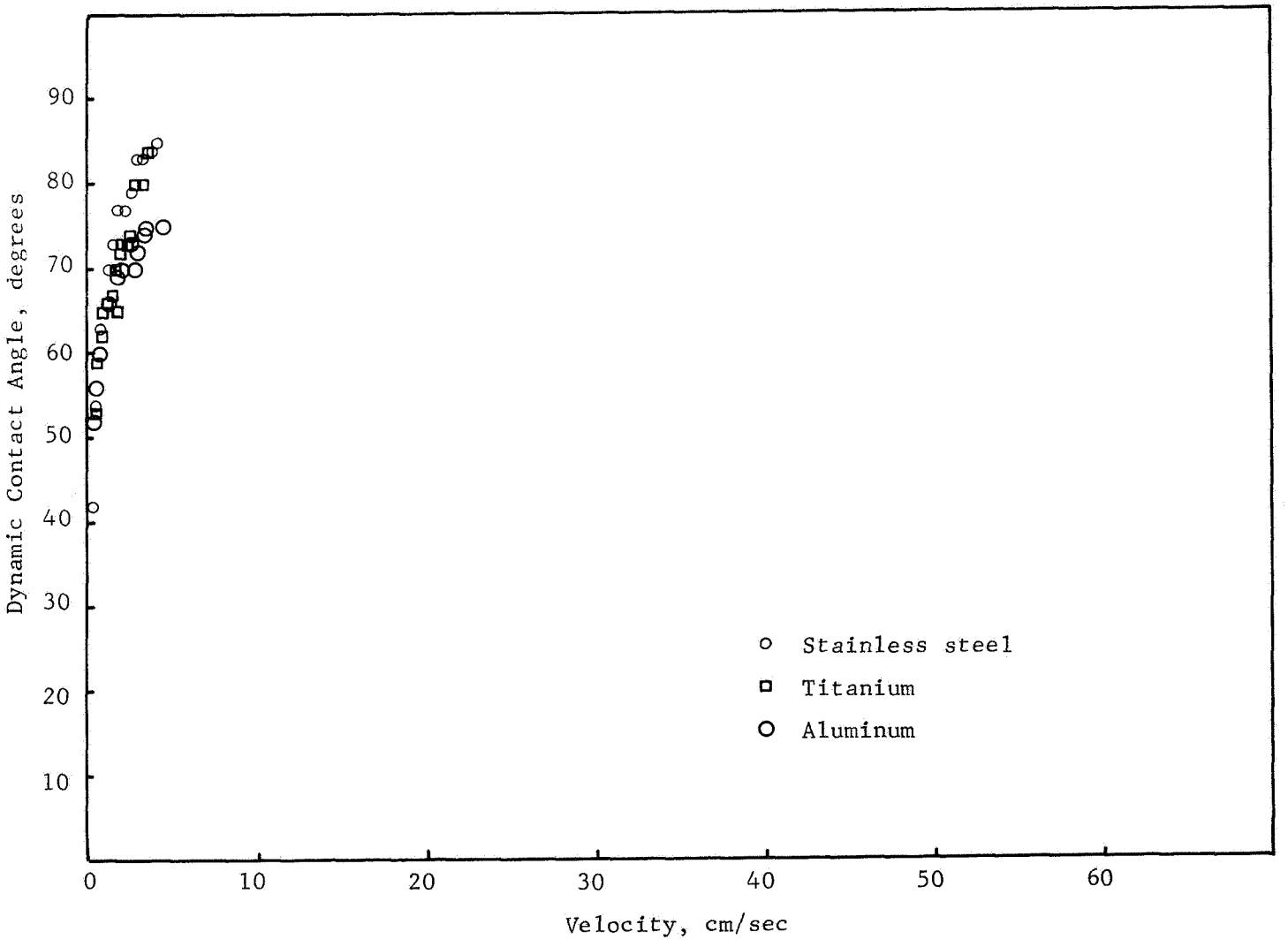

DISTRIBUTION LIST FOR FINAL REPORT

Contract NAS3-9705
NASA CR-72441

	Number of Copies
National Aeronautics and Space Administration Washington, D. C. 20546 Attn: RV-1/Warren Keller	2
NASA-Lewis Research Center 21000 Brookpark Road Cleveland, Ohio 44135	
Attn: Technology Utilization Office, MS 3-19	1
Technical Information Division, MS 5-5	1
Library, MS 60-3	2
Spacecraft Technology Division	
a. C. C. Conger, MS 54-1	1
b. E. W. Otto, MS 54-1	1
c. D. A. Petrash, MS 54-1	25
Report Control Office, MS 5-5	1
Agena & Support Procurement Section, MS 500-110	1
NASA Scientific and Technical Information Facility P. O. Box 33 College Park, Maryland 20740 Attn: NASA Representative RQT-2448	6
Southwest Research Institute 8500 Culebra Road San Antonio, Texas 78206 Attn: Dr. H. Norman Abramson	1
Dr. Marvin Adelberg 4043 Cody Road Sherman Oaks, California 91403	1
TRW Space Technology Laboratory One Space Park Redondo Beach, California 90278 Attn: Dr. Pravin Bhuta	1
Bell Aerosystems Buffalo, New York 14240 Attn: Minas Insanian	1

Advanced Technology Laboratories
General Electric Company
Schenectady, New York 12301
Attn: Mr. R. F. Gaertner 1

Massachusetts Institute of Technology
Cambridge, Massachusetts 02139
Attn: Dr. Peter Griffith 1

Midwest Research Institute
425 Volker Boulevard
Kansas City, Missouri 64110
Attn: Dr. Sheldon Levy 1

Astronautics/Propulsion
Martin Denver Division
Denver, Colorado 80201
Attn: Howard L. Paynter 1

Spacecraft Thermodynamics Department
Lockheed Missile & Space Company
Sunnyvale, California 94008
Attn: Dr. Hugh M. Satterlee 1

Mechanical Engineering Department
Tufts University
Medford, Massachusetts 02155
Attn: Dr. Lloyd Trefethen 1

Aerospace Corporation
P. O. Box 95085
Los Angeles, California 90045
Attn: Library Technical Documents Group 1

Westinghouse Astronuclear Laboratories
Electric Propulsion Laboratory
Pittsburgh, Pennsylvania 15234
Attn: H. W. Szymanowski 1

Heat Transfer and Thermodynamic Laboratory
University of Michigan
Ann Arbor, Michigan
Attn: Dr. John A. Clark 1

University of California
Los Angeles, California
Attn: Dr. K. E. Forster 1

University of Kentucky
Lexington, Kentucky
c/o College of Engineering
Attn: Dr. John H. Lienhard 1

University of Michigan
Ann Arbor, Michigan
Attn: Dr. H. Merte, Jr. 1

Marshall Space Flight Center
Huntsville, Alabama 35812
Attn: A. L. Worland 1

Department of Mechanical Engineering
New York University
New York, New York 10453
Attn: Dr. Novak Zuber 1

Marshall Space Flight Center
Huntsville, Alabama 35812
Attn: H. Trucks/R-P&VE-PTP 1

Southwest Research Institute
Department of Mechanical Sciences
8500 Culebra Road
San Antonio, Texas 78206
Attn: Dr. Daniel D. Kana 1

McDonnell-Douglas Corporation
3000 Ocean Park Boulevard
Santa Monica, California
Attn: J. B. Blackmon 1